



Article

Modelling of Indoor Air Quality and Thermal Comfort in Passive Buildings Subjected to External Warm Climate Conditions

Eusébio Conceição ^{1,2,*} , João Gomes ³, Maria Inês Conceição ⁴ , Margarida Conceição ⁴, Maria Manuela Lúcio ¹ and Hazim Awbi ⁵

¹ Faculdade de Ciências e Tecnologia, Universidade do Algarve, Campus de Gambelas, 8005-139 Faro, Portugal; maria.manuela.lucio@gmail.com

² ADAI, Departamento de Engenharia Mecânica, Rua Luís Reis Santos, Pólo II, 3030-788 Coimbra, Portugal

³ Instituto Superior de Engenharia, Universidade do Algarve, Campus da Penha, 8005-139 Faro, Portugal; jgomes@ualg.pt

⁴ Instituto Superior Técnico, Universidade de Lisboa, 1049-001 Lisboa, Portugal; ines.conceicao@tecnico.ulisboa.pt (M.I.C.); margarida.conceicao@tecnico.ulisboa.pt (M.C.)

⁵ School of Built Environment, University of Reading, Reading RG6 6AW, UK; h.b.awbi@reading.ac.uk

* Correspondence: econcei@ualg.pt

Abstract: Air renewal rate is an important parameter for both indoor air quality and thermal comfort. However, to improve indoor thermal comfort, the air renewal rate to be used, in general, will depend on the outdoor air temperature values. This article presents the modelling of indoor air quality and thermal comfort for occupants of a passive building subject to a climate with warm conditions. The ventilation and shading strategies implemented for the interior spaces are then considered, as well as the use of an underground space for storing cooled air. The indoor air quality is evaluated using the carbon dioxide concentration, and thermal comfort is evaluated using the Predicted Mean Vote index. The geometry of the passive building, with complex topology, is generated using a numerical model. The simulation is performed by Building Thermal Response software, considering the building's geometry and materials, ventilation, and occupancy, among others. The building studied is a circular auditorium. The auditorium is divided into four semi-circular auditoriums and a central circular space, with vertical glazed windows and horizontal shading devices on its entire outer surface. Typical summer conditions existing in a Mediterranean-type environment were considered. In this work, two cases were simulated: in Case 1, the occupation is verified in the central space and the four semi-circular auditoriums and all spaces are considered as one; in Case 2, the occupation is verified only in each semi-circular auditorium and each one works independently. For both cases, three strategies were applied: A, without shading and geothermal devices; B, with a geothermal device and without a shading device; and C, with both shading and geothermal devices. The airflow rate contributes to improving indoor air quality throughout the day and thermal comfort for occupants, especially in the morning. The geothermal and shading devices improve the thermal comfort level, mainly in the afternoon.

Keywords: indoor air quality; thermal comfort; passive buildings; numerical simulation



Citation: Conceição, E.; Gomes, J.; Conceição, M.I.; Conceição, M.; Lúcio, M.M.; Awbi, H. Modelling of Indoor Air Quality and Thermal Comfort in Passive Buildings Subjected to External Warm Climate Conditions. *Atmosphere* **2024**, *15*, 1282. <https://doi.org/10.3390/atmos15111282>

Academic Editors: Teodoro Georgiadis and Boris Igor Palella

Received: 4 August 2024

Revised: 13 October 2024

Accepted: 21 October 2024

Published: 25 October 2024



Copyright: © 2024 by the authors. Licensee MDPI, Basel, Switzerland. This article is an open access article distributed under the terms and conditions of the Creative Commons Attribution (CC BY) license (<https://creativecommons.org/licenses/by/4.0/>).

1. Introduction

The levels of thermal comfort (TC) and indoor air quality (IAQ) found in buildings are influenced by the ventilation process used [1]. IAQ depends fundamentally on the airflow rate provided by the implemented ventilation system, which improves with an increase in the airflow rate in the occupied area of the buildings [2]. However, the influence of the airflow rate on the TC level, in addition to its value, also depends on the outside air temperature [3,4]. In summer, when the outside air temperature is lower than the inside air temperature, the increase in airflow rate contributes to improving the occupants' TC conditions. On the other hand, the airflow rate should be decreased when the outside air

temperature is higher than the indoor air temperature. In this case, the IAQ level must be combined with the TC level to have the appropriate airflow rate.

The lowest outside air temperature is usually before sunrise, and the highest outside air temperature is often in the middle of the afternoon. In summer, it is important to consider the hours between sunset and sunrise, when the indoor air temperature is higher than the outdoor air temperature, to reduce the air temperature inside the building when it is unoccupied. It is also important to reduce the air temperature during the day when the building is occupied. Therefore, during the day and night, the indoor spaces of the building need to be ventilated. During the night or at midday, when there is no occupancy, the concept of air change rate is used, while during the day, in the morning and the afternoon, when there is occupancy, the concept of airflow rate is used. The first concept considers the number of air renewals per hour, while the second concept considers the airflow rate according to the number of people inside each indoor space of the building.

During the summer, in hot climates, it is important to choose the appropriate cooling strategy to use. The strategy must take into account the architecture of the building, its intended purpose, and its occupancy cycle. The option for passive or hybrid cooling strategies allows energy saving to be achieved simultaneously with the appropriate adjustment of TC conditions acceptable to the building's occupants [5–7]. Passive cooling strategies, such as night ventilation, solar shading devices, or a large stored cold thermal mass, can improve thermal comfort conditions for occupants in the hot season [8–11].

The use of passive strategies in buildings located in different climates and their contribution to energy saving [12,13] and the thermal comfort of occupants [13] have been the subjects of research over the last few years. Passive techniques, particularly in the cooling season, involve solar and heat protection solutions, solar control, the use of thermal mass, free cooling, and heat dissipation solutions [14]. The use of underground thermal storage is a rarely used passive technique, although a recent study demonstrates the effectiveness of its application for cooling a residence compartment located in a hot climate [15].

Underground spaces can be used to store geothermal energy in a wide range of climates, whether to provide heating or cooling. These types of spaces can have other uses, other than for human occupation, being temporarily used as thermal energy storage spaces. One aspect that should be taken into account when choosing them is their size (possible air storage volume) and their intended purpose. Spaces that are hot during the day but cool at night should be chosen, i.e., spaces that have a fairly high temperature difference between day and night. The choice of this type of space can be made in advance through numerical simulations based on knowledge of the external climate data existing in the region of the building under study.

This study uses geothermal energy stored underground as a possible cooling strategy (it can also be used as a strategy in the heating season). This space is well insulated from the outside environment, either by walls or by several layers of earth substrate. Both at night and during the day, this space is subject to a ventilation process by perfect mixing. This means that, at the entrance, the air mixes completely with the existing air and then leaves at the same temperature as the internal environment. This methodology can be provided by some internal fans to ensure that there will be no internal recirculation zones that could reduce the efficiency of the process. The calculation of the air change rate must be taken into account, whether for cooling or heating, to ensure that the process is carried out for the expected time.

Regarding the shading strategy used in this study, it was considered that this will occur in two phases, fixed horizontal shading and mobile shading during the day, in order to guarantee total shading. In any case, in practice, the shading system consists of a system of blinds installed on each window that is moved by controlled motors or simply by human action.

The ventilation system installed in this work is designed to cool the space at night. In the morning, as the air temperature in some spaces is higher than the air temperature

outside, ventilation is used to reduce the air temperature inside occupied spaces. During the middle of the day, there is no occupancy in indoor spaces, and the air temperature level outside is considerably higher than the indoor air temperature. Thus, the ventilation level is reduced to minimize the increase in internal air temperature. In the early afternoon, high outside air temperatures are registered. During these hours, the ventilation from an underground space, cooled during the night by geothermal energy, is used to cool the occupied spaces naturally.

Thus, the following points summarize the main innovations proposed in this work:

- Use of an underground space for storing cooled air;
- A shading strategy for interior spaces using adjustable shading devices;
- A ventilation strategy.

This article presents the work developed on a ventilation system installed in a circular auditorium. The auditorium is divided into four semi-circular zones and a central circular space. It is also provided with surrounding vertical windows and horizontal surrounding shading devices. The study considered warm climatic conditions (summer season), assuming the auditorium is located in a region characterized by a Mediterranean-type climate, namely the south of Portugal. Two cases were studied: one in which the occupation is verified in the central space and the four semi-circular auditoriums and all spaces work together, and the second in which the occupation is only in each semi-circular auditorium and each one works independently. For both cases, three strategies were also considered: the auditorium does not have geothermal and shading devices, the auditorium has only the geothermal device, and the auditorium has both geothermal and shading devices. The airflow rate improves the indoor air quality all day and the thermal comfort mainly in the morning periods. The geothermal and shading devices improve the thermal comfort level, mainly in the afternoon.

This work aims to assess the comfort and air quality levels to which a circular auditorium is subjected in summer conditions. The ventilation system is combined with a shading system and a geothermal system. The first system involves a set of horizontal louvres around the building, placed above the level of the windows. This type of system, with a length equal to the height of the windows, guarantees shading during the hours of the day with the highest levels of insolation. During the early morning and late afternoon, when the sun rises and sets, this shading system, equipped with hinges, can be used to reduce the thermal load during sunrise and sunset. The geothermal system, installed underneath the circular auditorium, stores a quantity of cool air to be used in the afternoon when the outside air temperature reaches its highest value.

2. Literature Review

The level of thermal comfort depends on a set of environmental variables and personal parameters. Fanger [16], through experimental studies, developed a model based on the balance equation in the human body. This model considers heat transfer by convection between the body and the surrounding environment, either by forced convection or natural convection. The former takes air velocity into account, while the latter considers air temperature. This model also considers heat transfer by evaporation and radiation between the body and the surrounding environment. The former considers relative humidity, while the latter considers mean radiant temperature. This model also considers the thermal insulation of clothing (using the clo variable to evaluate its level) and heat generation (using the met variable to assess the metabolism rate). Fanger proposed evaluating the thermal comfort level of occupants in conditioned environments using two indices: PMV (Predicted Mean Vote), which changes between -3 and 3 , and PPD (Predicted Percentage of Dissatisfied people) [16]. In the formulation of these indices, environmental variables were considered (such as indoor air temperature (t_a), indoor relative humidity (RH), mean radiant temperature (t_r), and relative air velocity (v_a)), as well as personal variables (such as metabolic rate and clothing insulation). These indices were adopted by international standards [17,18] to classify indoor environments occupied by people and their perceived

TC level. In ISO 7730 [18], this classification is made according to three categories: A, with the PMV being between -0.2 and $+0.2$; B, with the PMV being between -0.5 and $+0.5$; and C, with the PMV being between -0.7 and $+0.7$. The use of these indices to assess the thermal comfort of building occupants has become widespread in many articles published on this subject [19–22]. However, the use of the PMV index in warm climates has shown some drawbacks for accurately predicting TC conditions [23]. Several studies have pointed to differences between the values predicted by the PMV index and those corresponding to the thermal sensations attributed by the occupants [24–26]. To adjust for these differences, it was suggested in 2002, by Fanger and Toftum [27], to use a correction factor called the “expectancy factor”. According to these authors [27], the value of this expectation factor can vary between 0.5 and 1 depending on the ventilation system used and how long the warm season lasts annually. Since then, several articles have addressed the implementation of this expectancy factor in the most varied situations [28–30]. Consequently, adaptive comfort models have emerged that seek to incorporate the adaptive behaviours of occupants who, when exposed to situations of thermal discomfort, react in different ways to restore the conditions that guarantee their return to a state of thermal comfort [31]. For example, Yao et al. [32] proposed an adaptive model that allows for minimizing the impact of PMV index overestimation in warm climates. On the other hand, Zhang et al. [33] proposed an algorithm to improve the estimation of the adaptive coefficient present in the PMV model. Other types of adaptive comfort models can be found in Carlucci et al. [34].

Among other variables, assessing the level of air quality is associated with the level of contaminants inside occupied spaces. This concentration depends, among other things, on the airflow rate, the number of occupants and the volume of the space. The ASHRAE 62-1 standard [35] recommends the airflow rate as a function of the number of occupants in the space to be ventilated, considering the type of contaminant to be removed. The volume of the space influences the evolution of the concentration in the transient regime but does not influence the maximum value obtained. Regarding contaminants, according to the ASHRAE 62-1 standard [35], in occupied spaces, the concentration of carbon dioxide (CO_2) can be used as a reference for IAQ present in spaces occupied by people. This standard proposes a CO_2 concentration up to a limit of 1000 ppm as acceptable. The use of CO_2 concentration as a marker of the air quality offered to people in interior spaces of buildings is common in studies conducted by the most diverse authors on this subject. For example, studies on IAQ were carried out in school buildings [36–39], office buildings [40], and institutional buildings [41], among other types of buildings [42,43].

The use of solar radiation incident on glazed surfaces can represent a cost-free heating source for adjacent interior spaces and, therefore, contribute to improving the TC conditions of occupants during the heating season [44,45]. However, solar gains through glazed surfaces due to incident solar radiation must be reduced during the cooling season. In these circumstances, it is common to install outside horizontal shading devices above windows to control the entry of solar radiation into interior spaces [46–48]. In the northern hemisphere, in latitudes that cover the territory of Portugal, which are characterized by a Mediterranean-type climate, this device is very effective on transparent south-facing surfaces [49]. On surfaces facing east and west, when the sun is at a lower height, this device does not prevent all solar radiation from entering. In this situation, blinds or obstacles between the transparent surfaces and the sun are preferable [50].

Thermal energy storage can be used to support ventilation systems that condition the air in building compartments during the heating and cooling seasons [51]. In this work, a numerical simulation is carried out to test the possibility of using an underground space (located under the building) to store cooled air during the night that will be distributed throughout the building’s compartments during certain periods of the day. The aim is to implement this solution during the summer season, evaluating its potential contribution to reducing the interior air temperature of the compartments and improving the TC of its occupants.

The Building Thermal Response simulation tool is a fundamental way of understanding the evolution of air temperature fields and solar radiation through opaque and transparent bodies, the evolution of contaminant concentrations, the evolution of energy consumption, and the evaluation of IAQ and conditions TC in the building compartments, among other aspects. Applications of this type of simulation tool can be seen in research work carried out in buildings where passive ventilation systems [52,53], natural ventilation systems [54,55], and active ventilation systems [56] were used, as well as where the thermal environmental conditions and air quality [57] existing there were evaluated.

3. Building Thermal Response Methodology

In the study developed in this article, software called Building Thermal Response (BTR) is used, which was designed to analyze the thermal response of buildings with complex topology [58,59]. The BTR software is used to simulate the thermal behaviour of a circular amphitheatre with a complex topology.

The BTR software has been developed by the authors for more than two decades with the main objective of developing a specific tool, similar to a virtual laboratory, that considers the thermal behaviour of passive buildings using renewable energy and, consequently, can evaluate the conditions of thermal comfort and air quality to which people are subjected inside buildings [58–60]. This software considers tools that allow the development of the design of a building with complex topology, the simulation of external environmental conditions from a few experimental data, the thermal response of passive buildings taking into account a library of existing opaque and transparent surfaces, the simulation of external solar radiation taking into account the shading system existing in the building and the various elements existing in the atmosphere, and the evaluation of the thermal comfort conditions of the occupants and indoor air quality, among others. This software, in very specific case studies, communicates with other software, allowing very detailed and specific assessments to be carried out, such as the simulation of three-dimensional internal flow in the building's compartments (considering the presence of occupants and the assessment of internal air quality), unidirectional flow inside ventilation ducts (taking into account different ventilation systems), the simulation of human thermophysiology and clothing (considering the assessment of the level of thermal comfort and draught risk), and the acoustic response of buildings (considering the presence of binaural manikins), among additional added value. This last component of the software, which considers the coupling between different software applications, allows the exchange of data and geometry between them. This type of methodology allows the user to relatively quickly design a complex building using an innovative and rapid methodology to obtain a group of variables taking into account external climatic conditions, the use of renewable energy, construction, and human comfort.

3.1. Geometric Model

This section presents the geometric model used to represent the building consisting of a circular auditorium with particular characteristics. In this sense, CAD (Computer-Aided Design) software and GBD (Geometric Building Design) software were used. The GBD software was used to develop the geometry of the circular auditorium [60], while the CAD methodology was used to view the geometry of the circular auditorium. CAD methodologies are frequently applied in building design [61,62].

The circular auditorium presented in this work includes four semi-circular auditoriums and a central circular area (Figures 1 and 2). The semi-circular auditoriums can operate individually or together to form a single circular auditorium. Therefore, in this work, two study cases were defined as follows:

- Case 1: The building functions as a single circular auditorium, and the central circular area functions as a stage with seated people distributed across the four semi-circular auditoriums. Both central space and semi-circular auditoriums are occupied by people.

- Case 2: The circular central area functions as a passage space and people sit simultaneously in the four semi-circular auditoriums. In this case, only the semi-circular auditoriums are occupied, with the stage placed on the steps next to the central circular space.

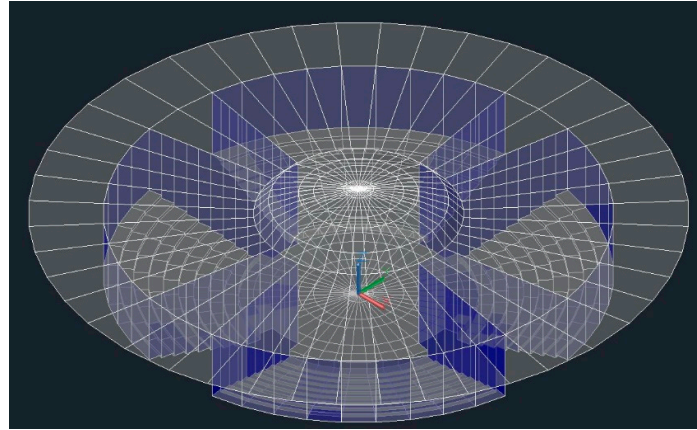


Figure 1. Three-dimensional view of the virtual circular auditorium, with the shading device. The blue color represents transparent surfaces and the gray color represents opaque surfaces.

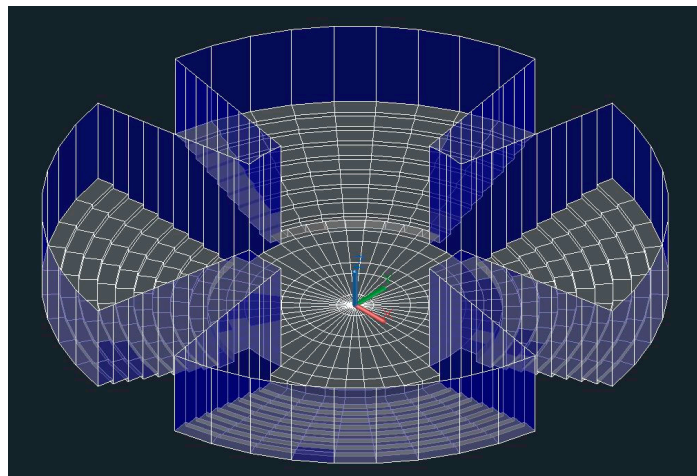


Figure 2. Three-dimensional view of the virtual circular auditorium, without the shading device. The blue color represents transparent surfaces and the gray color represents opaque surfaces.

In both cases, the following three strategies were applied:

- Strategy A: Without geothermal and shading devices;
- Strategy B: With a geothermal device and without a shading device;
- Strategy C: With geothermal and shading devices.

Between two semi-circular auditoriums, there is a corridor. It is used for people to enter through the central circular area into the respective semi-circular auditorium. The vertical walls surrounding each semi-circular auditorium, whether in contact with the outside environment or facing the corridor, are made of simple glass.

The ceiling of the circular auditorium is made of an opaque material and is divided into three parts (Figure 1):

- An inner part, at the top of the central circular area, with an ellipsoid configuration;
- A central part, above each semi-circular auditorium, with a flat horizontal configuration;
- An outer part, with a horizontal flat configuration. This part is articulated and can be positioned vertically in front of the windows, thus functioning as a shading device.

The solution used in this work, using the envelope built with glazed surfaces and the roof equipped with a shading system, guarantees good levels of interior luminosity, controlling the entry of solar radiation to reduce the thermal load on the occupied spaces.

The length of the shading system's louvres is equal to the height of the windows. This arrangement allows the blinds to be used as shutters. Three scenarios can therefore be achieved:

- Sunrise and sunset: During this period, east- or west-facing windows and the surrounding glazed surfaces are subject to direct solar radiation. Therefore, shade canopies are used in the closed position.
- Early morning and late afternoon: during this period, windows facing south-west and south-east, and the surrounding glazed surfaces, are subject to direct solar radiation; therefore, shade canopies are used in a partially closed position.
- Late morning and early afternoon: during this period, the main south-facing windows and the surrounding glazed surfaces are not subject to direct solar radiation due to the installed shading system.

This building is equipped with an underground space. Its volume is twice the volume corresponding to the occupied spaces of the circular auditorium. This type of space can operate as a thermal energy storage system as it is possible to store cold air at night to be used in the building's compartments during the day when the outside air temperature is higher. In this case, it will be used during the afternoon.

Figures 1 and 2 show three-dimensional views of the circular auditorium, respectively, with and without the shading device.

3.2. Mathematic Model

The numerical model present in the BTR software was presented and validated in the work developed by Conceição and Lúcio [63], having been applied over the years in different types of research studies involving the thermal behaviour of buildings [58,59,64]. BTR is software that works through an integral methodology. The mathematical model considers integral equations of mass and energy balance in the transient regime. The mathematical model is divided into two parts:

- One consisting of a system of mass balance integral equations, in a transient regime: The flows of water vapour and contaminants, in particular carbon dioxide, are considered for each space in the circular semi-auditorium and the central circular zone.
- Another consisting of a system of energy balance integral equations, in a transient regime, in which the model takes into account the floor of the circular central area, the floor of the circular semi-auditoriums, the ceiling of the circular auditorium, vertical transparent surfaces, and horizontal shading devices placed on top of the windows.

The mass and energy balance integral equations take into account heat conduction, mass and heat convection, mass diffusion, heat exchange by radiation, energy transport, mass adsorption and desorption, and heat evaporation, among others. They also consider the accumulation of heat and mass in the left-hand term and heat and mass flows, heat generation, etc., in the right-hand term.

An integral energy conservation equation is developed for each of the bodies that make up the building, namely, for each transparent body, for each layer of each opaque surface, for each layer of each interior body, and for each interior space. Also, an integral mass conservation equation is developed for each interior space and for each component. In this study, water vapour and CO₂ concentrations were considered. In the case of opaque and transparent bodies, integral mass conservation equations are also considered for the surfaces in contact with the external environment that represents the adsorption and desorption of water vapour on these surfaces. All equations work as a coupling system; that is, all equations have connections with neighbouring equations. This methodology ensures that all variables are dependent on neighbouring variables.

To solve the set of integral energy balance equations and integral mass balance equations generated by the software, the Runge–Kutta–Fehlberg method is used, in which the error is controlled in order to speed up the simulation time.

The following are verified in calculating the integral energy balance equations:

- Use of dimensionless coefficients in calculating heat dissipation that occurs through natural, forced, and mixed convection;
- The heat transfer by conduction is considered inside the opaque body layers;
- The radiative exchanges take into account the incident solar radiation, the solar radiation absorbed by glasses, and the solar radiation transmitted through the glass.

The following are verified in calculating the integral mass balance equations:

- Use of dimensionless coefficients in calculating mass transfer that occurs through natural, forced, and mixed convection;
- Use of Fick's law in calculating mass transfer by the diffusion phenomenon.

The following simplifications are considered in the former balances of the model:

- Disregard of non-uniformities existing in the distribution of temperatures throughout each body;
- One-dimensional treatment of conductive and convective heat fluxes through walls;
- Always writing the sensible heat storage term on the left-hand side and the heat flux terms on the right-hand side of the heat balance equations.

The PMV model depends on the environmental variables t_a , t_r , RH and v_a . This model depends on the thermal balance between heat generated in the body and the heat lost to the surrounding environment. In general, the heat lost to the environment depends on convective, conductive, evaporative, and radiative exchanges. In convective exchanges, t_a (calculated by BTR) is considered for natural convection, and v_a (calculated by BTR) is considered for forced convection. Conductive exchanges are verified, in most situations, through clothing. This heat is subsequently transferred to the outside through convection and radiation. Evaporative exchanges consider RH (calculated by BTR) and t_a (calculated by BTR). Finally, in radiative exchanges, including between surfaces and the human body, t_r (calculated by BTR) is considered.

In this study, the numerical model calculates the mean values of the environmental variables. As summer conditions are considered and low mean values of v_a in the occupied spaces are obtained, the local thermal discomfort phenomenon associated with the draught risk is not considered.

3.3. Initial and Boundary Conditions

In this type of simulation, in order to obtain a more realistic distribution of temperatures and contaminant concentrations in all the bodies considered in the building, average values are considered at the beginning of a day, and the previous 5 days are simulated. This methodology provides a more realistic distribution of temperatures and contaminant concentrations, which will be used at the beginning of the simulation process.

The external environment conditions, used as boundary conditions, namely the solar radiation, air temperature, air relative humidity, wind velocity, wind direction, and carbon dioxide concentration, are calculated numerically. The solar radiation is evaluated numerically during the simulation using the geometric solar equation.

The numerical evolutions of the boundary conditions are developed from experimental data measured by a meteorological station located near the building. In the case of air temperature and air relative humidity, the maximum and minimum values and the respective times when these values are obtained are considered and, from trigonometric equations, their daily evolutions are calculated numerically. In the case of wind velocity and wind direction, average values and standard deviations are calculated and, through random computational functions, the evolutions of these variables are generated numerically. In the case of CO₂ concentration, an average value measured experimentally in the region where the building is located is used. Since the real measurements present values

and fluctuations characteristic of the days corresponding to the simulations carried out, in this case, it was decided to consider a typical day representative of a clear summer day in the region where the building is located. The theoretical evolution thus obtained allows results to be obtained that are very close to the real ones, without considering the occurrence of possible fluctuations characteristic of specific climatic phenomena.

The external environmental conditions considered are the following:

- The air temperature varies between 21.1 °C at 5 a.m. and 34.8 °C at 3:30 p.m.; the fluctuation in the air temperature value, around the average value, is presented as a value of 1 °C;
- Relative air humidity varies between 32% at 5:17 am and 72% at 3:30 p.m.; the fluctuation in the value of relative air humidity, around the average value, is presented as a value of 5%;
- Air speed has an average value of 12 m/s, with a fluctuation of 11.2 m/s from its average value;
- The direction of air speed has an average value of 180° and a fluctuation of 135° from its average value.

The CO₂ concentration outside was considered to be 280 ppm.

3.4. Airflow

In warm climates, such as the Mediterranean climate, during the cooling season, namely from June to September, the variation in outside air temperature is significant and can fluctuate throughout the day by around 20 °C between early morning and the hottest time of day (around 2–3 p.m.). Therefore, in passive buildings, it is important to plan cooling strategies that allow for dealing with these significant changes in outside temperatures. These strategies may involve having variable airflow levels and using variable shading systems (like those mentioned in Section 3.2) that are adaptable to the outside environmental conditions throughout the day.

The airflow rate exchange between the outdoor and the occupied indoor spaces influences the level of air quality and thermal comfort [65–67]. However, considering variations in occupancy and outdoor environmental variables, the airflow rate needs to vary throughout the day. Therefore, this study considers four different regimes throughout the day:

- Regime that runs during the night: The air change rate used during the night is associated with cooling the occupied interior and the underground spaces when it is used. In this study, during the night and until sunrise, an air change rate of 10 per hour was used.
- Regime that takes place during the morning: During the day, an airflow rate was used that takes into account the number of occupants in the space (based on international standards). When the air temperature in indoor spaces is higher than the outdoor air temperature, as is the case in the morning, the airflow rate is doubled to reduce the air temperature in indoor spaces.
- Regime that takes place during the afternoon: During this period, the outside air temperature reaches very high values. However, the outdoor temperature continues to be higher than the indoor air temperature despite the additional thermal load due to the occupants. In this situation, an airflow rate was considered taking occupancy (based on international standards) into account. As an alternative to outside air, previously cooled air from the underground storage space can be used.
- Regime that takes place during midday: There is no occupancy at lunchtime. However, it is important to reduce the CO₂ concentration, but the outside air temperature is higher than the indoor air temperature. Therefore, only one air change was used.

In this study, in accordance with Portuguese standards [68], a ventilation rate of 35 m³/h per person was used.

In Case 1, during the ventilation process, the air is exchanged between the outdoor (or underground space) and each space (central circular space and semi-circular auditorium). In Case 2, during the ventilation process, the air is exchanged between the outdoor (or underground space) and the central circular space. From this central circular space, the airflow goes to the semi-circular auditoriums and, subsequently, to the outdoor environment.

The airflow topology is shown in Figure 3. Figure 3a refers to the topology used at night in both Cases 1 and 2. Figure 3b refers to the topology used during the morning, midday and afternoon (strategy A) for Case 1. Figure 3c refers to the topology used during the afternoon (strategies B and C) for Case 1. Figure 3d refers to the topology used during the morning, midday and afternoon (strategy A) for Case 2. Figure 3e refers to the topology used during the afternoon (strategies B and C) for Case 2.

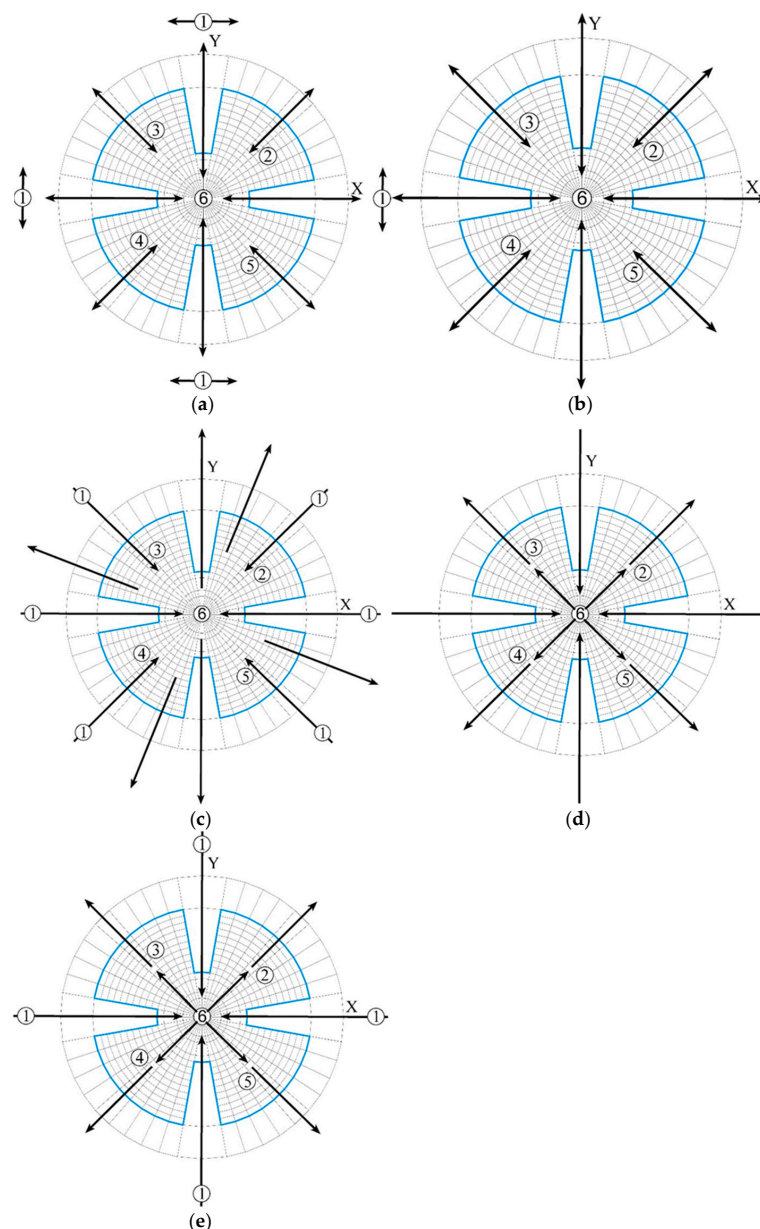


Figure 3. Airflow topology: (a) Cases 1 and 2 at night; (b) Case 1 during morning, midday and afternoon (strategies A and C); (c) Case 1 in afternoon (strategies B and C); (d) Case 2 during morning, midday and afternoon (strategies A and C); (e) Case 2 in afternoon (strategies B and C). The numbers represent the following: 1, outdoor space; 2, 3, 4 and 5, respectively, the semi-circular auditoriums 2, 3, 4 and 5; 6, central space.

The influence of the strategies implemented in the assessment of TC and IAQ levels will be analyzed and compared in Section 4. The spaces evaluated are those presented in Figure 3, and are renamed in Section 4 as follows: space 1 as OUT; space 2 as SA_2; space 3 as SA_3; space 4 as SA_4; space 5 as SA_5; and space 6 as SC_6.

3.5. Occupation

In this study, it was considered that occupation occurs in the morning and afternoon. The spaces are occupied in the morning between 8 am and 12 pm and in the afternoon between 2 pm and 6 pm. For each case, the occupancy level is as follows:

- Case 1: 24 people in each semi-circular auditorium and 12 people in the central space;
- Case 2: 27 people in each semi-circular auditorium.

3.6. Mesh Generation

When calculating the incident solar radiation, each surface is divided into smaller surfaces using a mesh. This calculation makes it possible to calculate, with greater precision, the incident, absorbed, and transmitted radiation on transparent surfaces and the incident and absorbed radiation on opaque surfaces.

3.6.1. Grid Independence

In this section, the grid's independence is evaluated. In this analysis, each surface is divided into several subsurfaces. Figure 4(1–4) show the mesh generation when the following subdivisions are applied: 1×1 ; 2×2 ; 3×3 ; 4×4 ; 5×5 ; 10×10 ; and 15×15 . This study consists of calculating the sum of the total incident radiation to which each surface is subjected when the horizontal shading device is applied.

As an example of the influence of mesh discretization on the calculation of total solar radiation, the evolution of the total solar radiation transmitted on the transparent surfaces for the different subdivisions of the surfaces (shown in Figure 4(1–4)) is presented in Figure 5.

According to the results shown in Figure 5, the 5×5 , 10×10 , and 15×15 subdivisions show good convergence between themselves. Regarding the option for the 5×5 subdivision, the differences in the 10×10 subdivision are, on average, -0.54% , while the differences in the 15×15 subdivision are, on average, -0.53% . The 3×3 and 4×4 subdivisions show slight discrepancies with the previous results, while the 1×1 and 2×2 subdivisions show large differences between the results. Therefore, the 5×5 subdivision was chosen because it presents a good compromise between the results.

3.6.2. Grid Applied in This Study

In this study, each surface is divided into at least 5×5 elements. All bodies have surfaces with a width and height and are formed by a trapezoid or a triangle. These surfaces, where the heat flow passes through the smallest thickness in a unidirectional manner, are divided into infinitesimal areas with trapezoidal or triangular configurations. In the centre of the circular zones, the surfaces are considered to be a set of concentric and juxtaposed triangles. These triangles are, in turn, divided into infinitesimal triangular areas.

Figure 6 shows the mesh generation used in a semi-circular auditorium and a quarter of the central space. In Figure 6a,b, the mesh generation is observed, respectively, without and with the ceiling and shading devices. In Figure 6, the lower area and side walls are represented in black and the ceiling and shading system are represented in magenta.

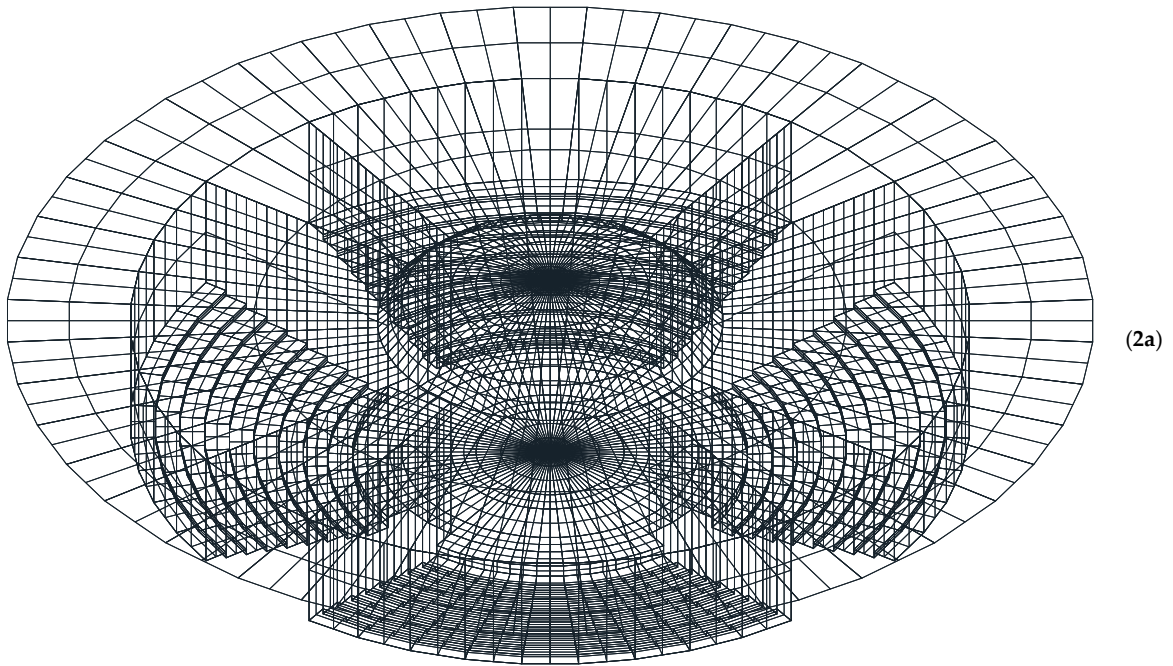
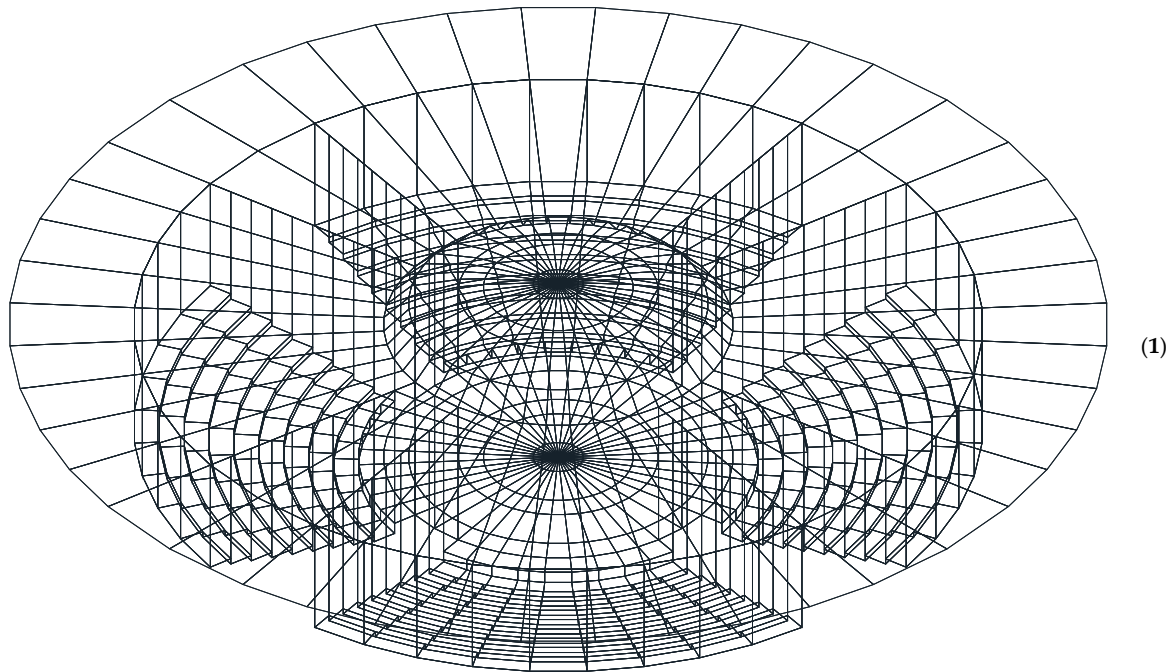


Figure 4. Cont.

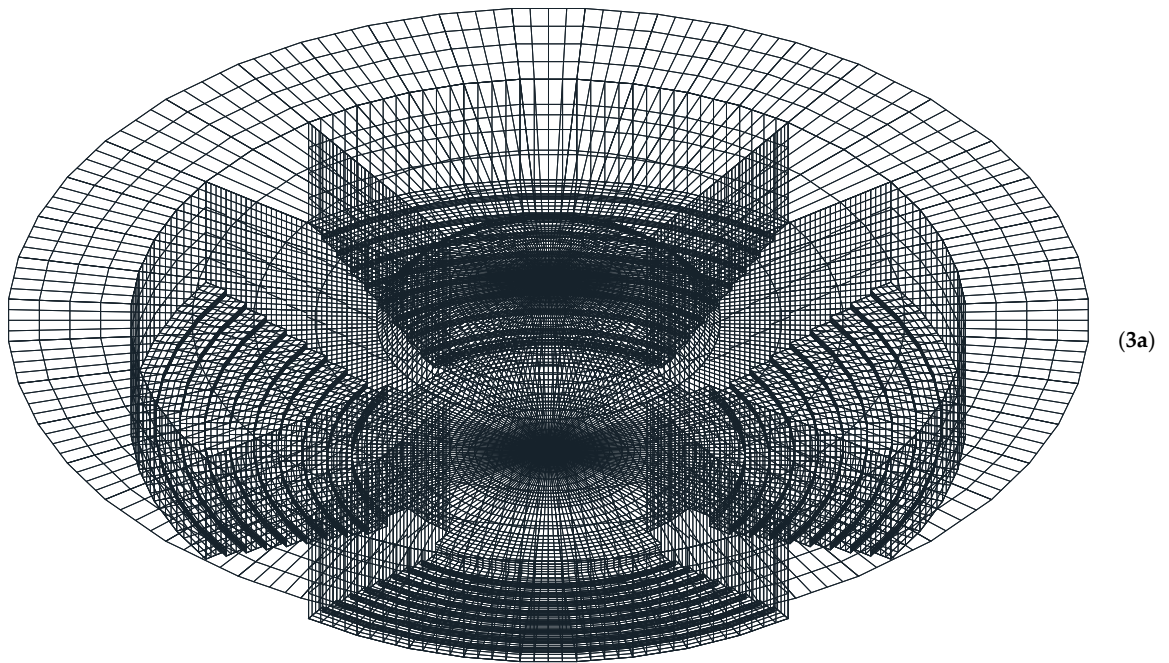
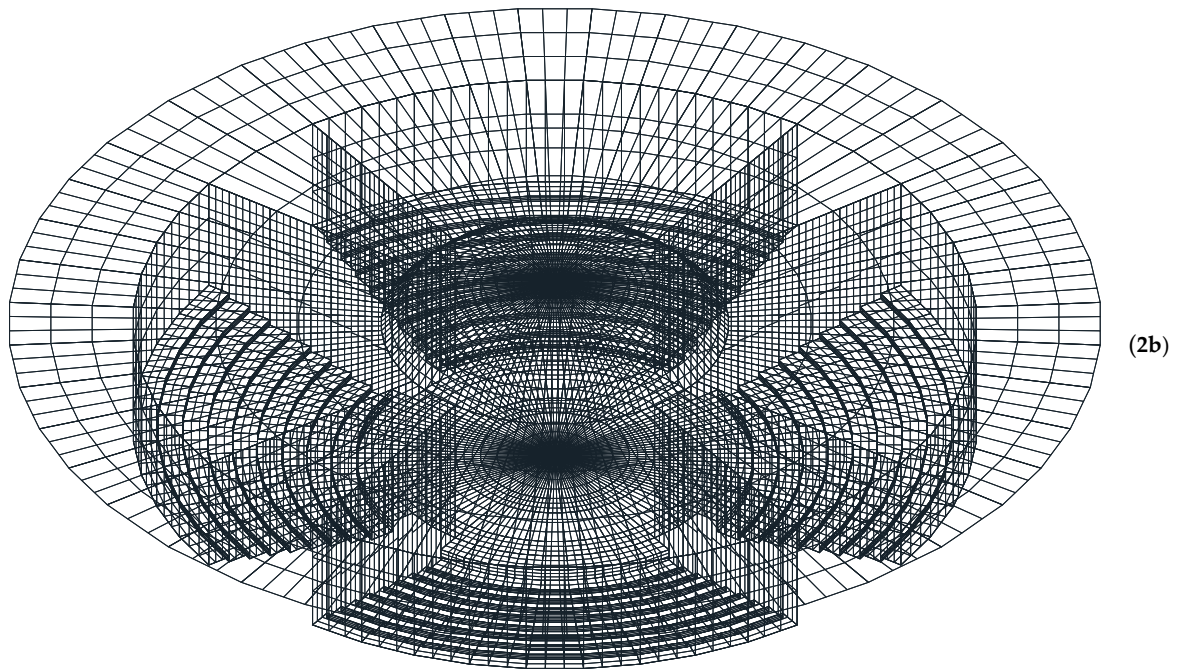


Figure 4. Cont.

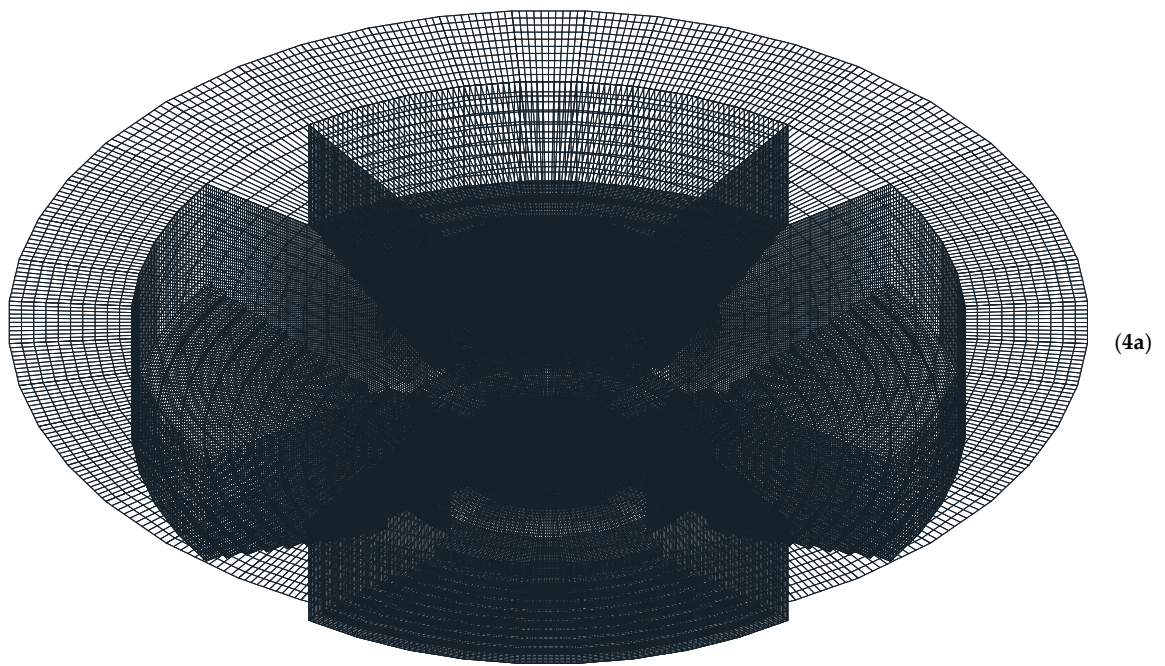
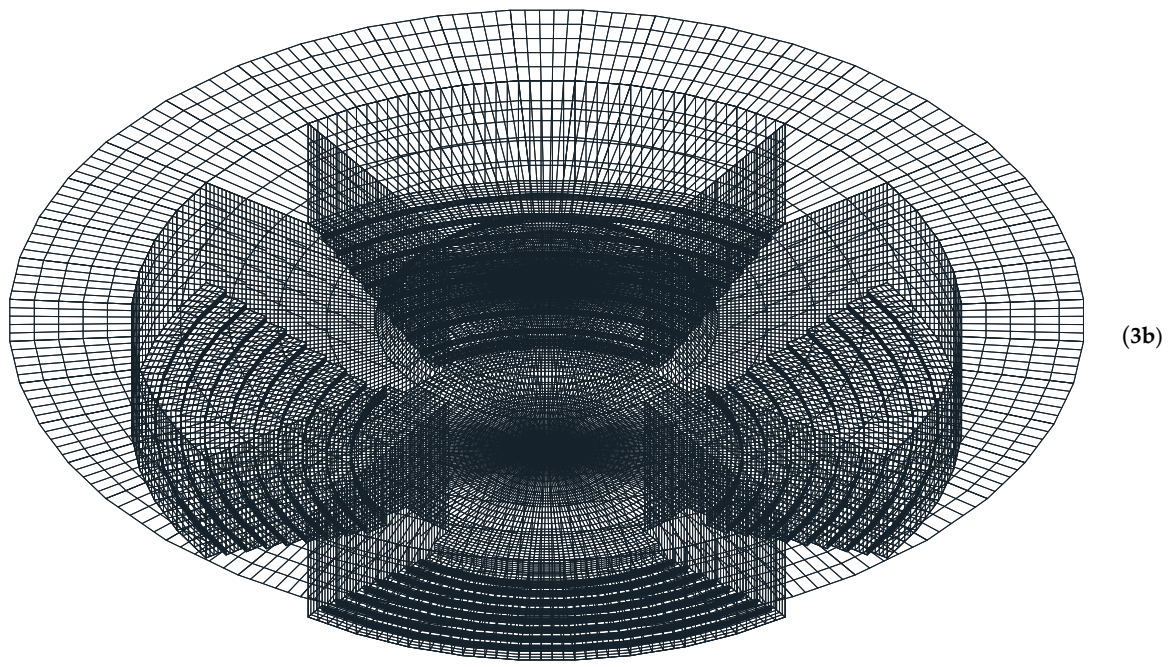


Figure 4. Cont.

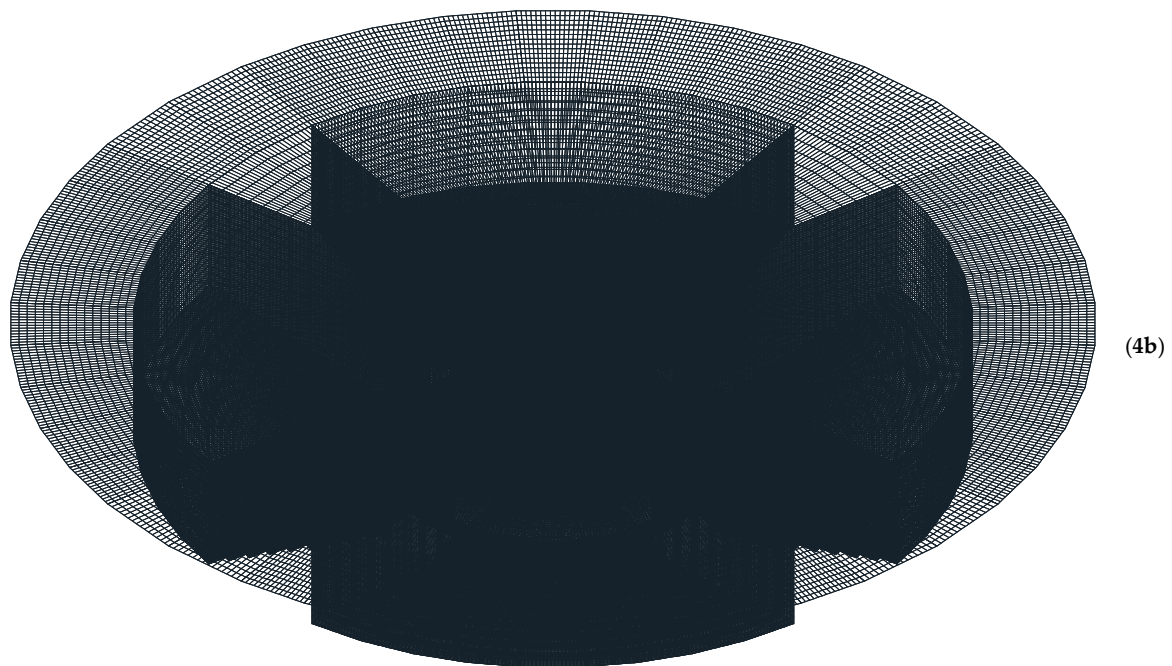


Figure 4. (1) Grid generation applied in the numerical simulations made for Case 1 when each surface is subdivided into 1×1 elements. (2) Grid generation applied in the numerical simulations made for Case 1 when each surface is subdivided into (a) 2×2 and (b) 3×3 elements. (3) Grid generation applied in the numerical simulations made for Case 1 when each surface is subdivided into (a) 4×4 and (b) 5×5 elements. (4) Grid generation applied in the numerical simulations made for Case 1 when each surface is subdivided into (a) 10×10 and (b) 15×15 elements.

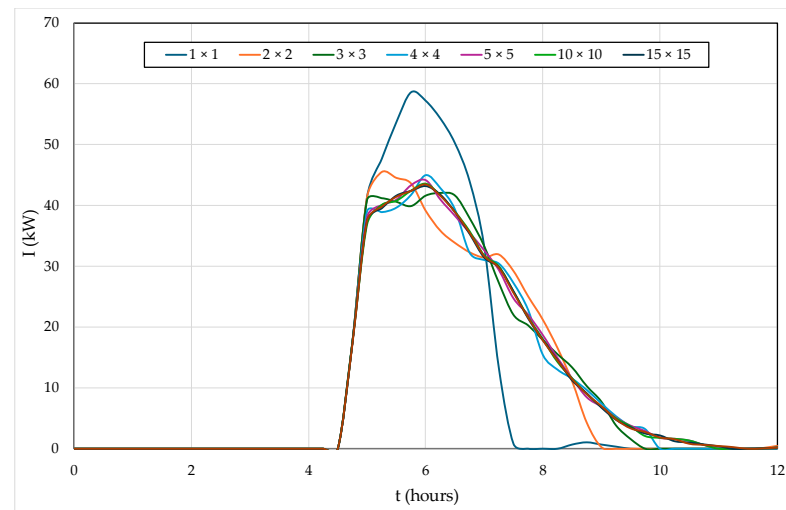


Figure 5. Evolution of the total solar radiation transmitted on the transparent surfaces for the different subdivisions of the surfaces (1×1 ; 2×2 ; 3×3 ; 4×4 ; 5×5 ; 10×10 ; 15×15).

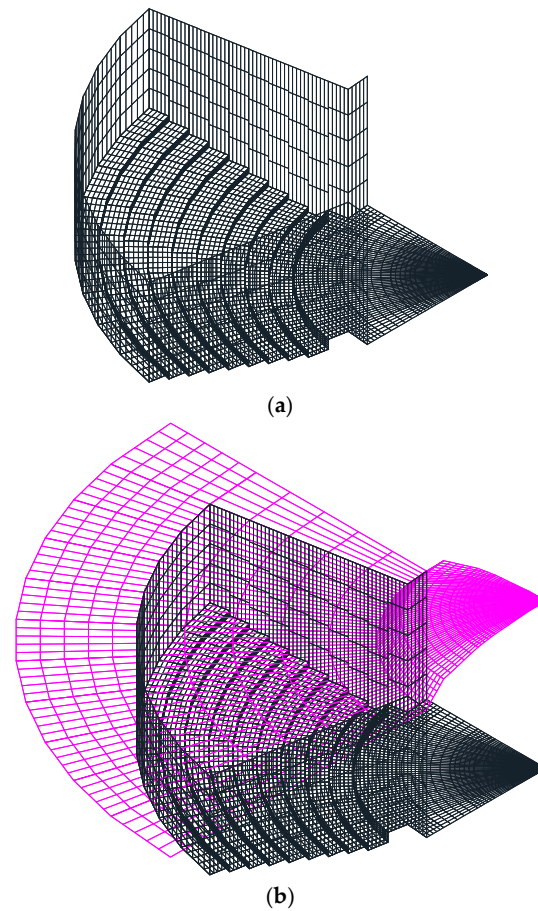


Figure 6. Mesh generation of a semi-circular auditorium (a) without and (b) with ceiling and shading devices. The lower area and side walls are represented in black and the ceiling and shading system are represented in magenta.

3.7. Materials

The circular auditorium was built with opaque and transparent surfaces. The opaque bodies are the roof, shading devices, floor, and ground. The number of layers considered in these bodies is as follows:

- Nine for the roof, used as a boundary with the external environment;
- Seven for the shading devices, used as a boundary with the external environment;
- Ten for the floor and ground, used as a border with the soil.

In the thermal analysis of the opaque surfaces, the following variables for each layer of these surfaces were considered:

- Thickness;
- Specific heat at constant pressure;
- Thermal conductivity;
- Specific mass.

When constructing the roof, the existence of gypsum board, insulation materials, cement, intermediate materials, wood, waterproof materials, and tiles was considered. It was considered that the shading device was made up of an aluminum structure. The layer near the floor presented a small thickness, while the layer far from the floor presented a larger thickness.

Thus, in this work, the numerical model calculates, inside each opaque body, the temperature of different layers using each one's thermal information. The obtained temperature distributions, in transient conditions, inside each opaque body are more representative of the real situation.

The transparent bodies are located around the auditorium and consist of windows and doors made of single glass pane. The thickness of this glass is 4 mm. These transparent bodies, used as a boundary with the external environment, are considered to be made of one layer.

In the thermal analysis of the transparent surfaces, the following variables for the layer of these surfaces were considered:

- Thickness;
- Specific heat at constant pressure;
- Thermal conductivity;
- Specific mass.

Thus, the numerical model calculates the temperature evolution of each transparent body using the thermal information of each body.

3.8. Model Validation

The numerical model was validated in steady-state and transient conditions using spaces of a real building and an experimental chamber. In steady-state conditions, the numerical model was validated in winter conditions in an experimental chamber that had a radiant floor system powered by a solar collector, one desk, and two seated experimental manikins [63]. According to Conceição and Lúcio [63], the comparison between the experimental and numerical results of the surrounding surface and internal temperatures was successfully guaranteed. In transient conditions, the numerical model was validated in a real school building for winter and summer conditions [69,70]. In both conditions, a comparison was made between the values of the temperature of the air inside a school building, under the effect of solar radiation, obtained experimentally, and those obtained numerically, the result of which was very similar.

4. Results and Discussion

This section presents the results obtained by the Building Thermal Response software used to evaluate the evolution of the CO₂, the indoor relative air velocity (v_a), the indoor air temperature (t_a), the indoor relative humidity (RH), the mean radiant temperature (t_r), and the PMV index verified in the studied building. The evolution of each of these variables is obtained in each of the spaces of the auditorium and corresponds to the average value calculated in the entire space in each time interval. The results are presented and discussed for Cases 1 and 2 and strategies A, B and C, considering their analysis separately.

In the following figures, referring to the results obtained, the analyzed spaces (marked in Figure 3) are identified as follows:

- Outdoor environment—OUT;
- Underground Air Storage Space—UASS;
- Semi-circular auditorium 2—SA_2;
- Semi-circular auditorium 3—SA_3;
- Semi-circular auditorium 4—SA_4;
- Semi-circular Auditorium 5—SA_5;
- Central space 6—SC_6.

4.1. Carbon Dioxide Concentration

Figure 7 presents the evolution of CO₂ to which occupants are subjected in the circular semi-auditoriums and the central space. Figure 7a refers to Case 1 and Figure 7b refers to Case 2.

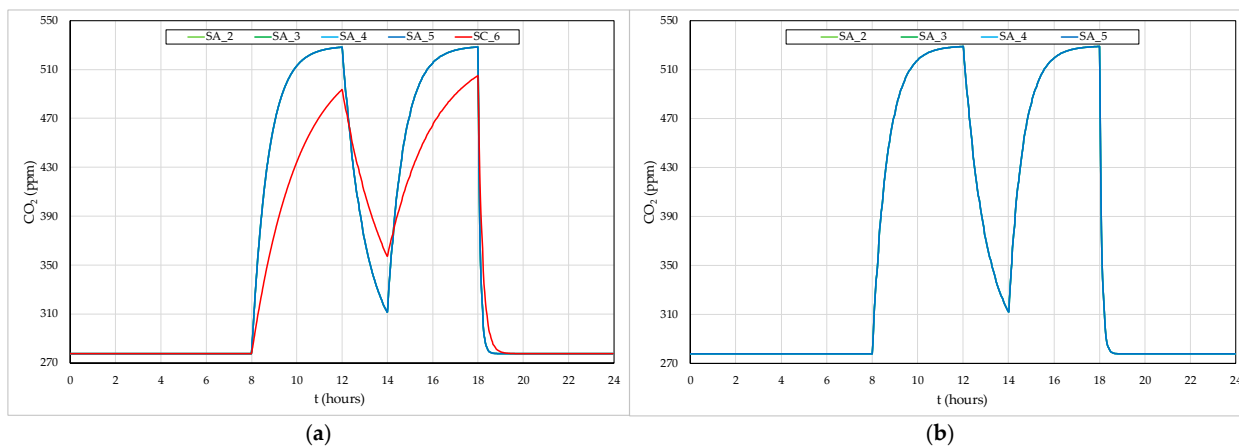


Figure 7. Average evolution of CO₂ to which occupants are subjected in the circular semi-auditoriums and in the central space: (a) Case 1; (b) Case 2.

As the occupation is the same in the spaces and the volume of the spaces is equal, the evolution of CO₂ concentration in the four semi-circular auditoriums is also equal. In Case 1, the CO₂ concentration is lower in the central circular space than in the semi-circular auditoriums. However, in all occupied spaces evaluated, the airflow rate is sufficient to promote an acceptable level of IAQ [35]. The CO₂ concentration in the semi-circular auditoriums is slightly higher in Case 2 than in Case 1.

The airflow rate during the night, in both cases, is sufficient to eliminate all indoor CO₂ concentrations. However, the airflow rate during lunchtime is not sufficient to eliminate all CO₂ concentrations in the spaces.

The evolution of CO₂ concentration depends on the airflow rate and the volume of the space. The airflow rate influences the maximum value of the CO₂ concentration, and the volume influences the evolution of the CO₂ concentration. In this study, the semi-circular auditoriums and the central circular spaces do not reach the maximum CO₂ concentration during the day. This is due to the occupancy time being only 4 h in the morning and 4 h in the afternoon, and after vacating the spaces, the airflow rate is used to reduce the level of CO₂ concentration.

In general, the CO₂ concentration values in Cases 1 and 2 are similar. However, in Case 2, the difference in the CO₂ concentration in the central compartment and outside is zero because this space is not occupied.

4.2. Indoor Air Velocity

Table 1 presents the average v_a obtained in the circular semi-auditoriums and the central space for Cases 1 and 2. Note that in Table 1 the columns corresponding to the period of occupation of the semi-circular auditoriums are marked by a green zone.

Table 1. Average v_a (m/s) obtained in the circular semi-auditoriums and the central space for Cases 1 and 2. Period of occupation of the semi-circular auditoriums are marked by a green zone.

Case	Spaces	Time Period				
		0:00 to 8:00	8:00 to 12:00	12:00 to 14:00	14:00 to 18:00	18:00 to 24:00
1	SA_2 to SA_5	0.225	0.245	0.031	0.245	0.225
	SC_6	0.889	0.135	0.125	0.135	0.889
2	SA_2 to SA_5	1.346	0.271	0.187	0.271	1.346
	SC_6	0.993	0.890	0.138	0.890	0.993

The results show that the indoor v_a values depend on the ventilation process and directly on the airflow rate value used (see Section 3.4). During the occupancy period (between 8 and 12 h and between 14 and 18 h) of the semi-circular auditoriums, the IAV is slightly higher (about 10%) in Case 2 than in Case 1. During the non-occupancy period of the semi-circular auditoriums, the indoor v_a is significantly higher (about 600%) in Case 2 than in Case 1, which contributes to better cooling of these spaces.

4.3. Indoor Air Temperature

This section presents the evolution of t_a in the auditorium spaces and the outdoor environment. Figures 8–10 refer, respectively, to strategies A, B and C used in Case 1 (point a) and Case 2 (point b). Note that the orientations of the exterior facades of the semi-circular auditoriums are as follows: 2, the facade facing northeast; 3, the facade facing northwest; 4, the facade facing southwest; and 5, the facade facing southeast.

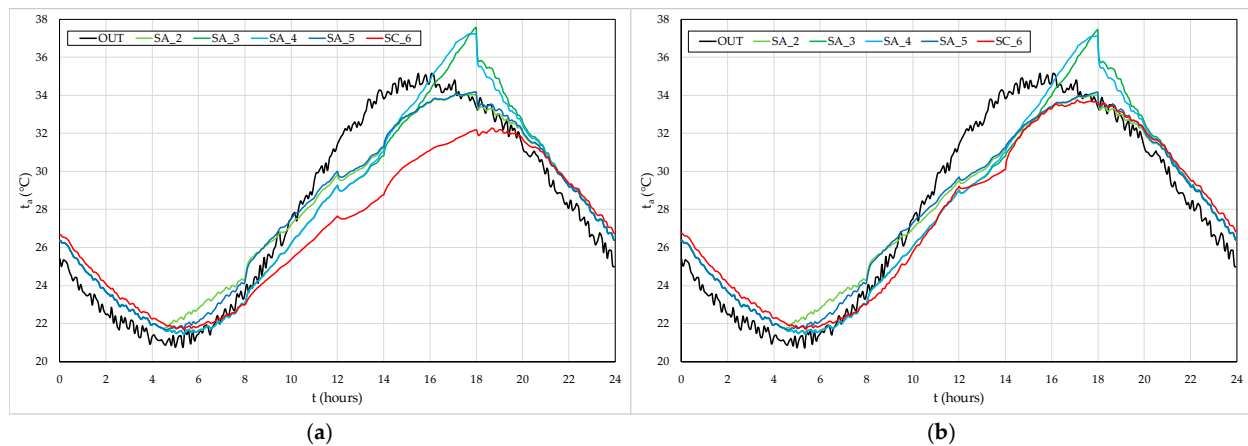


Figure 8. Average evolution of the outside temperature and indoor t_a in each space of the auditorium when using strategy A: (a) Case 1; (b) Case 2.

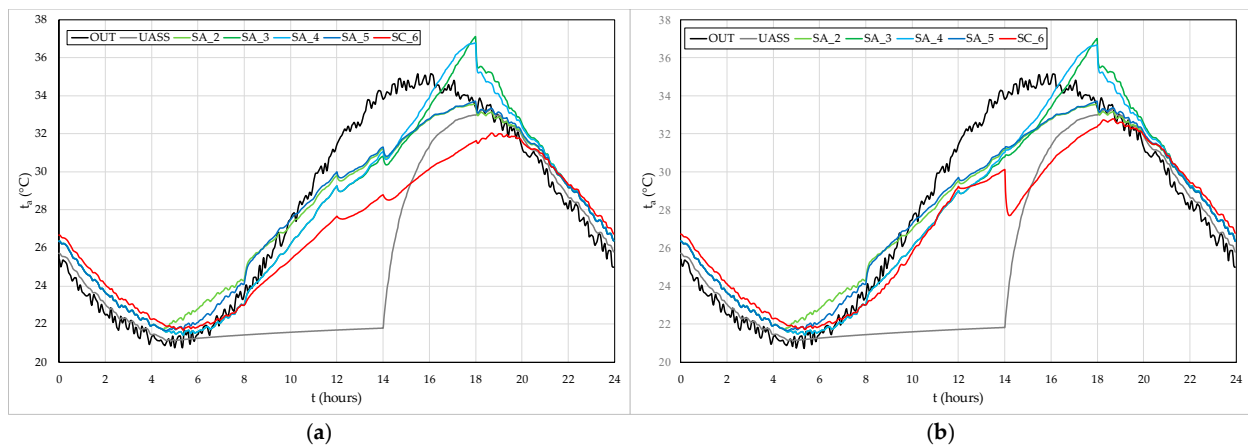


Figure 9. Average evolution of the outside temperature and indoor t_a in each space of the auditorium when using strategy B: (a) Case 1; (b) Case 2.

Before sunrise, when the lowest values of the outdoor air temperature are verified, an air change rate of 10 per hour is used to reduce the value of the air temperature in the indoor environment. When the higher values of outdoor air temperature are verified, seen in the early afternoon, the airflow rate (based on the occupancy) is used to avoid increasing the value of indoor air temperature.

Solar radiation transmitted through the glass, the generation of heat caused by the occupation of spaces, and the transmission of energy caused by the airflow rate in interior spaces are the most important factors in the variation in air temperature in interior spaces.

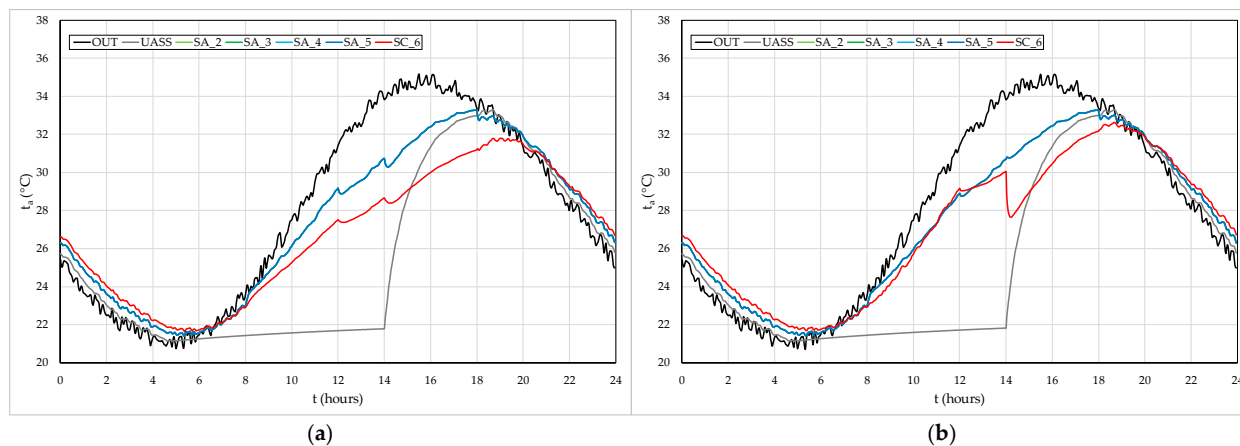


Figure 10. Average evolution of the outside temperature and indoor t_a in each space of the auditorium and in the underground storage space when using strategy C: (a) Case 1; (b) Case 2.

The horizontal shading system used ensures compartment shading in the late morning and early afternoon. However, in the early morning and late afternoon, when the sun height is lower, the shading system, when placed horizontally, allows some solar radiation to enter through the glazed surfaces. Therefore, the indoor t_a value in semi-circular auditoriums 2 and 5 increases in the early morning, and the indoor t_a value in semi-circular auditoriums 3 and 4 increases in the late afternoon.

During the morning and afternoon, the existence of occupants in the semi-circular auditoriums and the central space (only in Case 1) contributes to the increase in indoor t_a in these spaces. This is due to the generation of heat produced by the human body.

The transfer of energy, from the outdoor to the indoor environments and consequently from the indoor environment to the outdoor environment, through forced ventilation, allows the indoor t_a value to be reduced in the compartments in the following situations:

- During the night, air change is used to reduce the CO_2 concentration and, mainly, to reduce the indoor t_a value in all compartments to levels very close to the air temperature value in the outside environment.
- During the morning, the air change is used so that the indoor t_a value in the interior spaces, mainly in semi-circular auditoriums 2 and 5, is limited to the value of the air temperature in the outdoor environment. Therefore, the increase in the indoor t_a value is smaller than the increase in the air temperature in the outdoor environment and, at around 12 h, the indoor t_a values in all compartments are lower than the air temperature value in the outdoor environment.
- During lunchtime, on the one hand, the air change used allows for a reduction in the concentration of CO_2 in the spaces to be occupied during the afternoon, and on the other hand, it does not allow for a significant increase in the indoor t_a value.
- In the afternoon, taking into account the high outdoor air temperature, the value of the air change is reduced so that the indoor t_a value does not increase excessively, taking into account the need to maintain the indoor t_a within the acceptable limit.

Taking into account the increase in air temperature in interior spaces in the afternoon, mainly in semi-circular auditoriums 2 and 5, the use of underground spaces was implemented to store cooled air during the night to be used in part of the afternoon (see strategies B and C). As presented in Figures 9 and 10, the underground space (UASS) stores cool from the moment the indoor t_a value in this space becomes lower than the outside air temperature until the beginning of the afternoon. The cool air stored in the interior air of this space, whose temperature value is around 22 °C, when transferred to the interior spaces of the auditorium allows for a slight reduction in the indoor t_a value in these spaces in the afternoon.

In order to reduce the solar thermal load to which the compartments are subjected, in the early morning and late afternoon, in strategy C, a horizontal shading system is used, with the possibility of being adjustable. In this situation, as none of the semi-circular auditoriums are subject to solar thermal load and the occupancy is the same, the indoor t_a value is the same in the four semi-circular auditoriums. As presented in Figure 8, the use of this shading system slightly reduces the indoor t_a value in the central circular space (Case 1). Additionally, it significantly reduces the indoor t_a value in the semi-circular auditoriums in the morning and, mainly, in the afternoon.

During the day, in general, the indoor t_a in semi-circular auditoriums, in both Cases 1 and 2, shows similar values. However, in strategy A, the indoor t_a value in the central circular space is greater in Case 2 than in Case 1. On the other hand, in strategies B and C, the indoor t_a value in the central circular space is greater in Case 1 than in Case 2. The indoor t_a behaviour observed in both situations is due to the airflow in the central circular space being greater in Case 2 than in Case 1: in the first situation, the airflow coming from the outside environment increases the indoor t_a , while in the second situation, the airflow coming from the underground storage space decreases the indoor t_a .

During the night, in general, the indoor t_a values in the semi-circular auditoriums and in the central circular space, in both Cases 1 and 2, present similar values.

4.4. Indoor Relative Humidity

This section presents the evolution of RH in the auditorium spaces and the outdoor environment. Figures 11–13 refer, respectively, to strategies A, B and C used in Case 1 (point a) and Case 2 (point b).

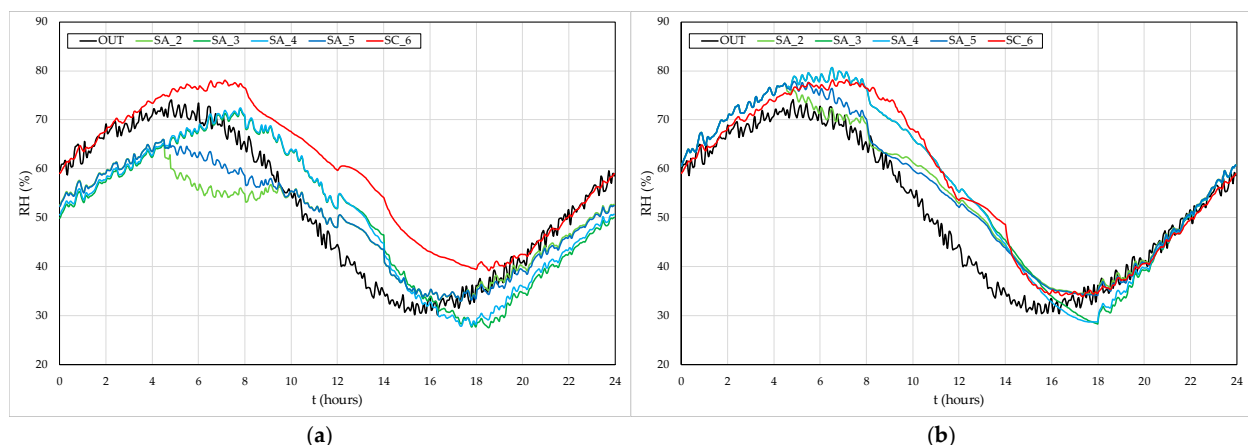


Figure 11. Average evolution of the outside relative humidity and indoor RH in each space of the auditorium when using strategy A: (a) Case 1; (b) Case 2.

As expected, the evolution of indoor RH has an inverse evolution to that of indoor t_a ; that is, the highest indoor RH values coincide with the lowest indoor t_a values and the lowest indoor RH values coincide with the highest IAT values.

When strategy A is used for Case 1, during the occupancy period, the highest indoor RH values are reached in spaces SA_3 and SA_4, with a value of approximately 70%, in the early morning (around 8 h); the lowest indoor RH values are reached in spaces SA_3 and SA_4, with a value of approximately 28%, in the late afternoon (around 18 h). Compared to Case 1, in Case 2, the indoor RH evolution values are slightly higher in all semi-circular auditoriums. In Case 2, during the occupancy period, the highest indoor RH values are reached in spaces SA_3 and SA_4, with a value of approximately 76%, in the early morning (around 8 h); the lowest indoor RH values are reached in the same spaces, SA_3 and SA_4, with a value of approximately 29%, in the late afternoon (around 18 h).

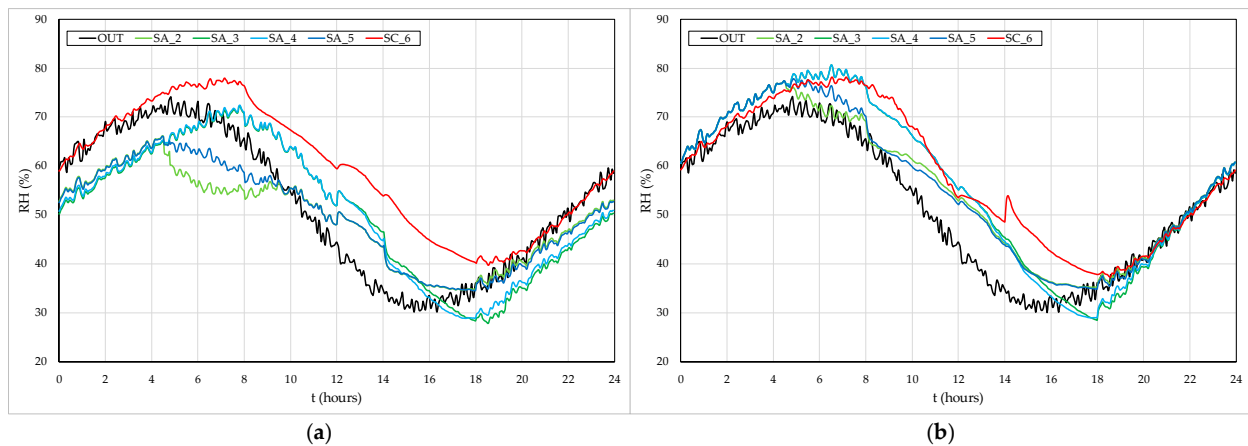


Figure 12. Average evolution of the outside relative humidity and indoor RH in each space of the auditorium when using strategy B: (a) Case 1; (b) Case 2.

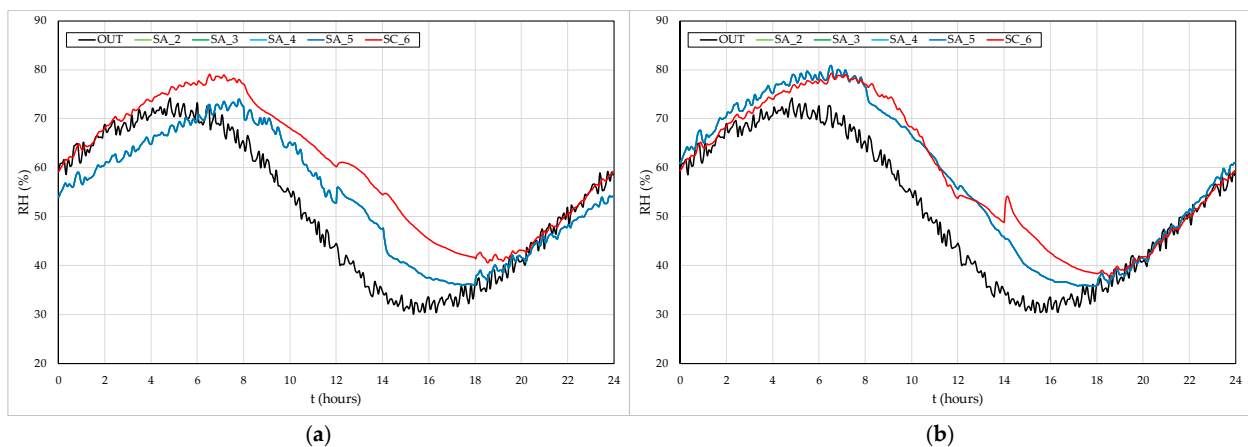


Figure 13. Average evolution of the outside relative humidity and indoor RH in each space of the auditorium when using strategy C: (a) Case 1; (b) Case 2.

When strategy B is used, the behaviour of the indoor RH evolution observed for both Cases 1 and 2 is very similar to that obtained when strategy A is used.

When strategy C is used, the evolution of the indoor RH observed for both Cases 1 and 2 presents higher values than those obtained when using strategies A and B. It is also verified, in both Cases 1 and 2, that the evolution of the indoor RH is the same in all semi-circular auditoriums, as was also verified for the evolution of the indoor t_a when using strategy C. In Case 1, during the occupancy period, the highest indoor RH values are approximately 72%, reached in the early morning (around 8 h), and the lowest indoor RH values are approximately 36%, reached in the late afternoon (around 18 h). Compared to Case 1, in Case 2, the indoor RH evolution values are slightly higher in all semi-circular auditoriums. In Case 2, during the occupancy period, the highest indoor RH values are approximately 77%, reached in the early morning (around 8 h), and the lowest indoor RH values are 38%, reached in the late afternoon (around 18 h).

4.5. Mean Radiant Temperature

The thermal comfort level depends not only on the indoor t_a values but also on the mean radiant temperature (t_r) values. Thus, this section presents the evolution of t_r in Figures 14–16, referring, respectively, to strategies A, B and C used in Case 1 (point a) and Case 2 (point b). The mean radiant temperature, t_r , is approximately calculated from the mean temperature of the surrounding surfaces [71,72], where these temperatures are weighted according to the area of these surfaces assuming a unitary value of emissivity.

The value obtained represents an average estimate of the t_r in the space considered, representative of the centre of the space. In order to more accurately assess the value of the t_r to which each occupant is subject, it will be necessary to take into account the geometry of the surrounding space, the emissivity of each surrounding surface, the real position of each occupant in the space, the geometry of each occupant, and the temperature field of the surrounding space.

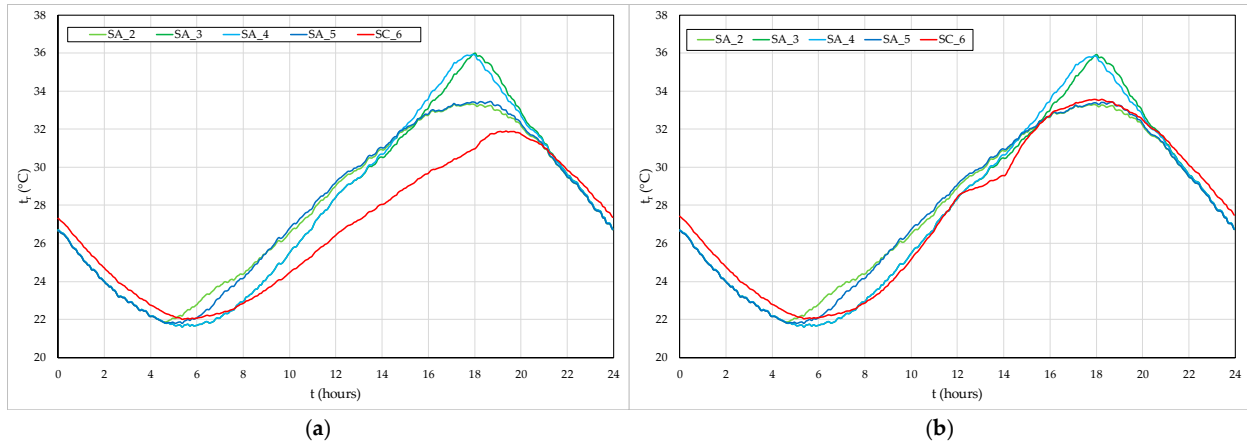


Figure 14. Average evolution of the t_r in each space of the auditorium when using strategy A: (a) Case 1; (b) Case 2.

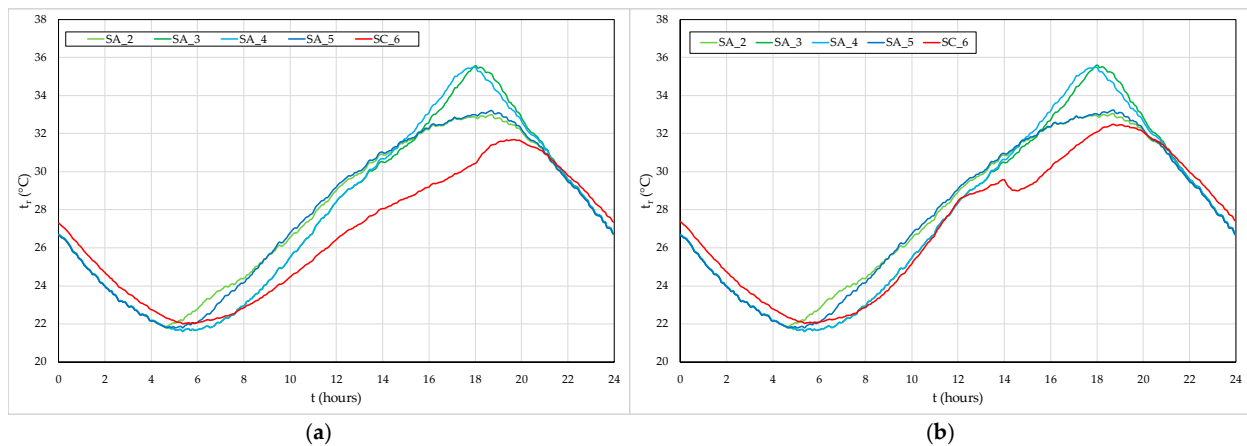


Figure 15. Average evolution of the t_r in each space of the auditorium when using strategy B: (a) Case 1; (b) Case 2.

In semi-circular auditoriums, the following is generally observed:

- The indoor t_a value is greater than the t_r value mainly when the space is occupied and when the compartments are subject to incident solar radiation on their transparent surfaces, in the early morning and late afternoon. In this case, the indoor t_a value contributes more than the t_r value to the increase in the value of the PMV index. This is due to the heating of the air in interior spaces caused either by the heat generated by the occupants or by solar radiation transmitted through transparent surfaces.
- During the night and lunchtime, the indoor t_a and t_r values are similar. This is due to the uniformity of indoor t_a values and the temperatures of the surrounding surfaces.

The surrounding surfaces of the central circular space (SC_6, Case 1) are not subject to the transmission of solar radiation into the interior. In addition to the heat generated by the occupants, this space is subject to heat exchange with the surrounding surfaces, namely the roof and the surfaces of the semi-circular auditoriums. During the day, the indoor t_a value is slightly higher than the t_r value, while the opposite is true at night. During the day,

this is due to the generation of internal heat caused by the occupants, while at night, this is due to the cooling of the interior air promoted by the flow of recirculating air from the outside environment.

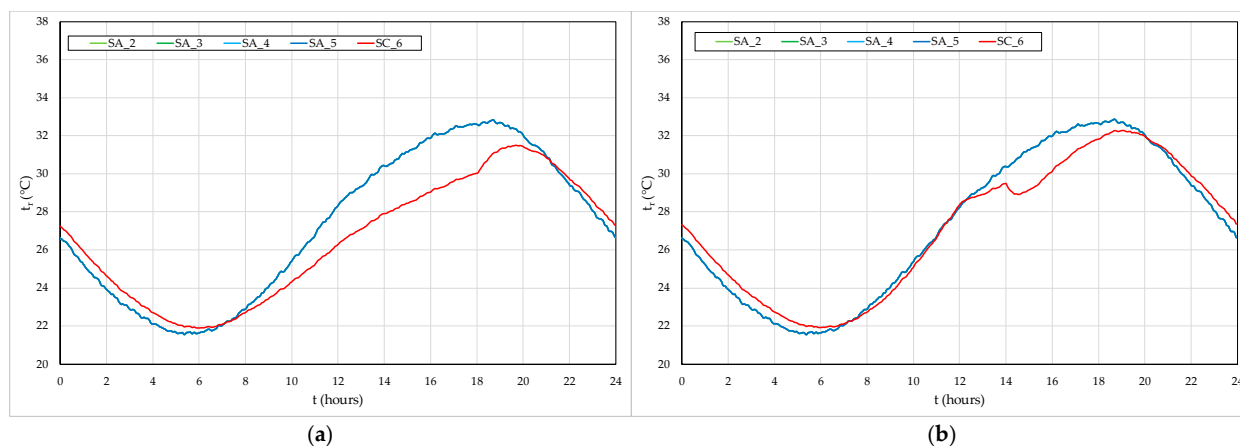


Figure 16. Average evolution of the t_r in each space of the auditorium when using strategy C: (a) Case 1; (b) Case 2.

During the day, for strategies A, B and C, the t_r value is approximately the same in the semi-circular auditoriums and is higher in Case 2 than in Case 1 in the central circular space. This is due to the airflow rate in the central circular space in Case 2 being greater than in Case 1. In strategies B and C, when the airflow in the central circular space comes from the underground storage space, in Case 2, the t_r value decreases slightly. However, it is not enough to be lower than the t_r value obtained in Case 1, due to the high increase that occurs in the morning, when the central circular space is ventilated with air from the outside environment.

4.6. Predicted Mean Vote Index

This section presents the evolution of the PMV index in the auditorium spaces. Figures 17–19 refer, respectively, to strategies A, B and C used in Case 1 (point a) and Case 2 (point b). The PMV was obtained from the methodology presented in ISO 7730 [18]. It depends on the environmental variables t_a , RH, t_a and v_a (whose evolution over time is calculated numerically by the software in each space of the auditorium) and on the parameters relating to the metabolic activity (in this study, 1.2 met [18], a typical value for seated people) and the level of clothing insulation (in this study, 0.5 clo, a value considered typical for a summer day in the region). The acceptable TC level, according to international standards [18], is associated with PMV index values between -0.7 and 0.7 (category C, [18]); negative values refer to the thermal comfort in cooler situations and positive values refer to the thermal comfort in warmer situations.

According to Figure 17 (strategy A), in the early morning, the highest PMV index is found in the semi-circular auditoriums located to the east (SA_2 and SA_5). Furthermore, the semi-circular auditorium located to the northeast (SA_2) presents slightly higher values than the semi-circular auditorium located to the southeast (SA_5). This is due to the incident solar radiation in these spaces at sunrise. During the morning, with ventilation and occupancy in these two compartments, similar PMV values are obtained, remaining as the compartments with the highest PMV indexes among all compartments. Throughout the morning, the lowest PMV index value is registered in the central circular space (SC_6), mainly in Case 1.

In the early afternoon (beginning of occupancy), the highest PMV index value is found in the semi-circular auditoriums facing east (SA_2 and SA_5); in the late afternoon, the highest PMV index value is found in the semi-circular auditoriums facing west (SA_3 and SA_4). In the late afternoon, due to the influence of solar radiation, the PMV index value

of semi-circular auditorium SA_4 is higher than the PMV index value of semi-circular auditorium SA_3. Throughout the afternoon, the lowest PMV index value is obtained in the central circular space (SC_6), mainly in Case 1.

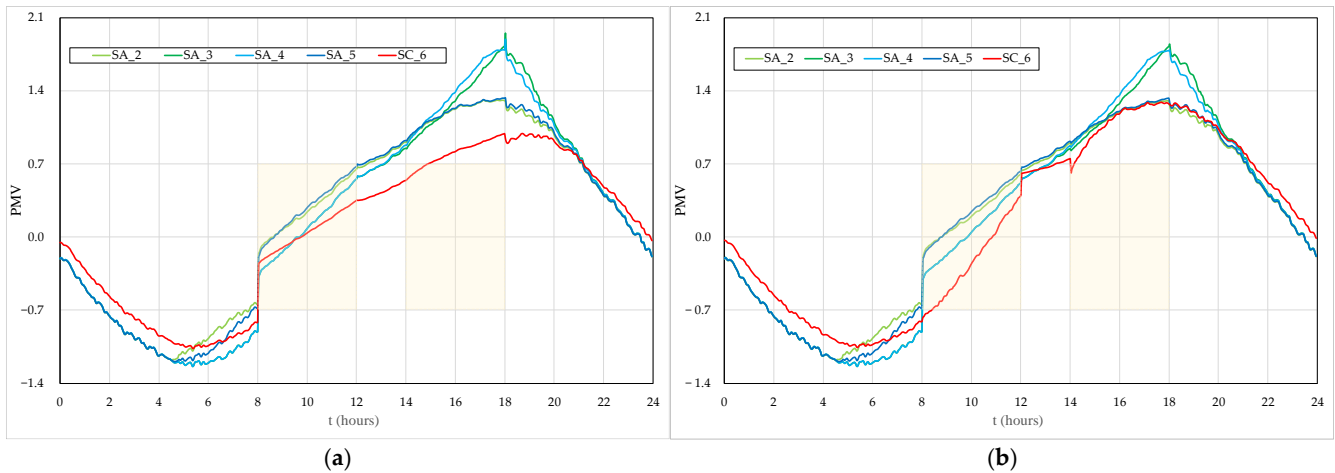


Figure 17. Average evolution of the PMV index in each space of the auditorium when using strategy A: (a) Case 1; (b) Case 2. The shaded zone defines the thermal comfort zone considered for the occupants (category C [18]).

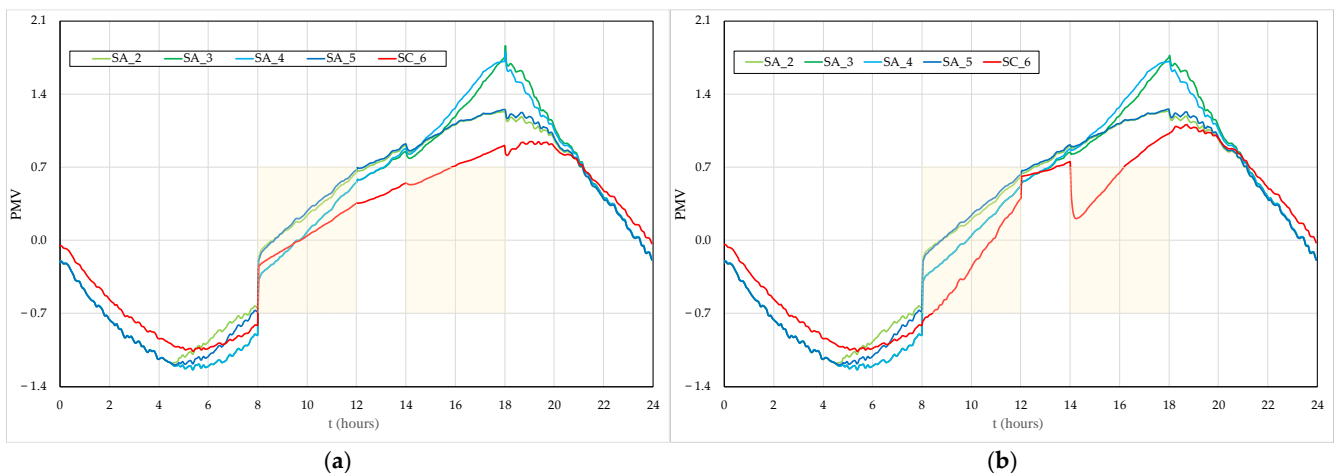


Figure 18. Average evolution of the PMV index in each space of the auditorium when using strategy B: (a) Case 1; (b) Case 2. The shaded zone defines the thermal comfort zone considered for the occupants (category C [18]).

In all compartments, the value of the PMV index increases from the beginning to the end of occupancy. During the morning, the TC level is acceptable due to essentially positive values of the PMV index in compartments SA_2 and SA_5, negative values until around mid-morning, and positive values in the remaining compartments. In the afternoon, the PMV index values increase, moving away from the acceptable level, despite the thermal comfort level in compartment SC_6 being close to the value considered acceptable. Throughout the afternoon, the TC level in the compartments is considered unacceptable due to the positive values of the PMV index.

When strategy B is implemented (Figure 18), the TC level obtained in the morning is similar to that obtained during the same period when strategy A is implemented. However, in the afternoon, the use of cooled air in the space of underground storage allows, in general, for a slight improvement in the TC level compared to that observed during the same period when strategy A is implemented.

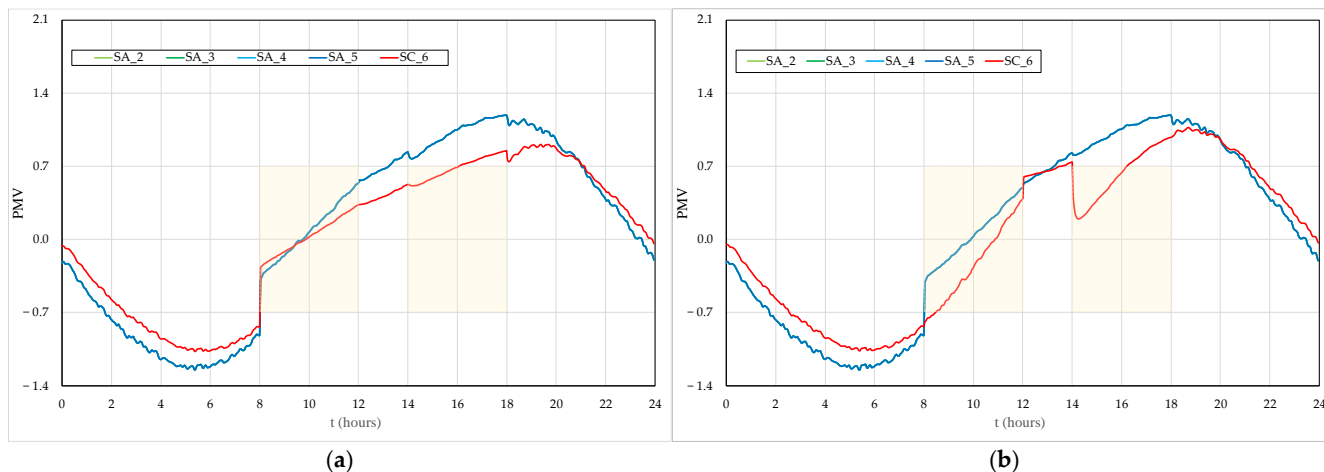


Figure 19. Average evolution of the PMV index in each space of the auditorium when using strategy C: (a) Case 1; (b) Case 2. The shaded zone defines the thermal comfort zone considered for the occupants (category C [18]).

When strategy C is implemented (Figure 19), the TC level obtained improves more clearly in the semi-circular auditoriums, remaining practically unchanged in the central circular space (SC_6).

Therefore, the TC level obtained when using strategy B presents improvements in relation to the one obtained when using strategy A. On the other hand, the TC level obtained when using strategy C presents improvements regarding the one obtained when using strategy B. In all strategies used, the TC level is acceptable in the morning. However, in the afternoon, the TC level obtained in the central circular space (SC_6, Case 1), when using strategy C, presents acceptable values until mid-afternoon and then values very close to the acceptable level. During this period, semi-circular auditoriums present, in turn, TC levels close to the acceptable level. The results obtained in Case 1, in general, are better than those obtained in Case 2.

Semi-circular auditoriums present, in general, for strategies A, B and C, similar levels of TC in both Cases 1 and 2. However, the central circular space presents four distinct situations concerning thermal TC level:

- During the night, in general, for strategies A, B and C, TC levels are similar in both Cases 1 and 2.
- In the morning, in general, for strategies A, B and C, the PMV index values are higher in Case 1 than in Case 2. This is due to the central circular space being occupied in Case 1 and unoccupied in Case 2. On the other hand, the central circular space is subject to higher levels of air velocity in Case 2 (with higher levels of ventilation) than in Case 1.
- During lunchtime, in general, for strategies A, B and C, the PMV index values are higher in Case 2 than in Case 1.
- In the afternoon, in general, for strategy A, the PMV index values are higher in Case 2 than in Case 1, while for strategies B and C it is observed that the PMV index values are higher in Case 1 than in Case 2.

5. Discussion

This study suggests that the implementation of passive cooling solutions in buildings can contribute to improving the thermal comfort of occupants, in line with the findings obtained in other similar studies [11,73,74]. The results showed that the use of underground spaces can contribute to the storage of thermal energy for later use, as proven by Alkargoly et al. [15]. However, during the afternoon, the implemented shading system is not sufficient to maintain the thermal comfort of the occupants within acceptable limits, so the implementation of additional passive solutions should be considered. These solutions may

involve improving the insulation of the external envelope [75] or designing a roof with more efficient heat dissipation [76].

The application of horizontal shading systems will be important mainly on south-facing facades, as they are not very efficient on east and west facades in the early and late hours of the day. To overcome this drawback, adjustable shading systems are used. This type of system can be controlled mechanically or, more simply, operated by the user. In this case, most of the east-facing shading systems are closed in the morning, while most of the west-facing shading systems are closed in the afternoon. The application of thermal energy storage (cooled air or heated air depending on the season) in underground spaces, preferably located below the building, is a possibility that should be considered and properly evaluated. In this case, it is important to efficiently control ventilation so that the system stores most of the energy at night and manages the consumption of thermal energy in the compartments during the day. In this way, it will be possible to take advantage of the energy storage capacity of the underground space in order to obtain maximum efficiency from the entire system.

In general, the advantages of this system are the use of renewable energy sources and the consequent savings in energy and related economic costs. The main disadvantage of this type of system is that it is less effective than a Heating, Ventilation and Air Conditioning (HVAC) system because it depends on solar radiation. The shading system using blinds has the advantage of being adjustable and not allowing heat to pass through direct radiation; however, it allows heat to enter through convection and conduction phenomena. The geothermal system takes advantage of the storage capacity of cold night air; however, it has the disadvantages of high initial investment and heat losses that occur throughout the day in storage.

The use of the strategies implemented in this study allows for savings in the consumption of fossil fuel energy because it essentially uses solar energy. Therefore, it also contributes to a reduction in greenhouse gas emissions and to better environmental sustainability. Underground spaces for energy storage can also be used during the heating season, thus contributing to the thermal comfort of occupants and energy savings throughout the year. However, during the cooling season, it is not possible to guarantee thermal comfort conditions for occupants throughout the day with the strategies implemented here alone. One possible solution is to reduce the occupancy hours, coinciding with the periods of the day when conditions that guarantee acceptable thermal comfort levels are obtained.

In summer conditions, it will be important to develop models to control shading systems in order to ensure the minimum passage of direct solar radiation through the windows, while maintaining the maximum passage of diffuse solar radiation in order to provide good levels of visual comfort to the occupants. This methodology consists of ensuring the maximum opening of the shading systems or, alternatively, placing horizontal systems that rotate around a vertical axis.

In winter conditions, it will be important to use shading systems that allow the entry of most of the solar radiation and to implement a ventilation system that allows the transfer of airflow from warmer areas to colder areas, where more energy is needed. In this case, it will be important to ensure air change rates that can guarantee good IAQ levels for the occupants.

6. Conclusions

This numerical study presented the modelling of indoor air quality and thermal comfort for occupants of a passive building subject to a climate with warm conditions. IAQ was evaluated by CO₂ concentration and thermal comfort was evaluated by PMV index.

In this study, two possible uses of the circular building were considered: Case 1 involved four occupied semi-circular auditoriums with a central space; Case 2 considered four occupied semi-circular auditoriums only. For both cases, three passive strategies were implemented: A, without shading and geothermal devices; B, with geothermal devices and without shading devices; and C, with both shading and geothermal devices.

For Case 1, the CO₂ concentration due to occupancy is lower in the central circular space than in the semi-circular auditoriums. In these compartments, the airflow rate used is sufficient to provide an acceptable level of IAQ throughout the occupancy cycle. The CO₂ concentration in the semi-circular auditoriums is slightly higher in Case 2 than in Case 1, although it remains within the acceptable level for IAQ. The airflow rate used during the night is sufficient to reduce all CO₂ concentrations inside the compartments. However, the airflow rate used at lunchtime is not sufficient to reduce all CO₂ concentrations inside the compartments.

According to the values obtained for the PMV index, the TC level of the occupants when using strategy B improves compared to that when using strategy A. On the other hand, the use of strategy C allows improvements in the TC level of occupants compared to that using strategy B.

During the entire morning occupancy period, whether strategy A, B or C is used, the TC level is acceptable, with PMV index values between -0.7 and $+0.7$. During the entire afternoon occupancy period, when strategy C is used, the TC level is only acceptable, for positive values of the PMV index up to $+0.7$, for approximately half of this period in the central circular space. In semi-circular auditoriums, whatever strategy (A, B or C) is used, TC levels are close to the acceptable limit (i.e., positive values of the PMV index). Therefore, these compartments have slightly warm indoor environmental conditions.

The semi-circular auditoriums present, in general, for strategies A, B and C, similar levels of TC in both Cases 1 and 2. During the night in the central circular space, in general, the TC levels are similar for both Cases 1 and 2. In this central circular space, during the morning and lunchtime interval, in general, the PMV index values are higher in Case 1 than in Case 2, regardless of whether strategy A, B or C is used. During the afternoon, in general, the PMV index values are higher in Case 2 than in Case 1 for strategy A and are higher in Case 1 than in Case 2 for strategies B and C.

The main limitations of this study are the insufficient capacity of the underground energy storage system to provide cool air to the spaces during their occupancy period, in addition to the heat losses that occur during the day in storage. Another limitation is the influence that solar radiation has on the thermal behaviour of the building, especially during the afternoon when the shading device system is less efficient in minimizing the entry of solar radiation through the windows. Regarding future work, it is proposed to implement an automatic control system that acts on the shading devices in order to make them more efficient in preventing the entry of direct solar radiation into the interior spaces throughout the day. Another future endeavour is to evaluate how the system studied in this work can be efficiently implemented during the heating season.

Author Contributions: E.C., J.G., M.I.C., M.C., M.M.L. and H.A. contributed equally to the design of the work, numerical simulation, analysis of results, and writing and review of the manuscript. All authors have read and agreed to the published version of the manuscript.

Funding: The authors would like to acknowledge the project SAICT-ALG/39586/2018, <https://doi.org/10.54499/SAICT-ALG/39586/2018>, from the Algarve Regional Operational Program (CRESC Algarve 2020), under the PORTUGAL 2020 Partnership Agreement, through the European Regional Development Fund (ERDF) and the National Science and Technology Foundation (FCT).

Institutional Review Board Statement: Not applicable.

Informed Consent Statement: Not applicable.

Data Availability Statement: Data is contained within the article.

Acknowledgments: The authors also would like to acknowledge the project UIDB/50022/2020, <https://doi.org/54499/UIDB/50022/2020>, under the National Science and Technology Foundation (FCT).

Conflicts of Interest: The authors declare no conflicts of interest.

Nomenclature

Abbreviations

BTR	Building Thermal Response
CAD	Computer-Aided Design
GBD	Geometric Building Design
IAQ	indoor air quality
OUT	outdoor;
PMV	Predicted Mean Vote
PPD	Predicted Percentage of Dissatisfied people
SA	semi-circular auditorium
SC	central space
TC	thermal comfort
UASS	Underground Air Storage Space.

Symbols

CO ₂	carbon dioxide concentration (ppm)
RH	relative humidity (%)
t	time (h)
t _a	air temperature (°C)
t _r	mean radiant temperature (°C)
v _a	relative air velocity (m/s)

References

1. Toyinbo, O. Indoor Environmental Quality, Pupils' Health, and Academic Performance—A Literature Review. *Buildings* **2023**, *13*, 2172. [[CrossRef](#)]
2. Rizzo, K.; Camilleri, M.; Gatt, D.; Yousif, C. Optimising Mechanical Ventilation for Indoor Air Quality and Thermal Comfort in a Mediterranean School Building. *Sustainability* **2024**, *16*, 766. [[CrossRef](#)]
3. Bian, F.; Chong, H.; Ding, C.; Zhang, W.; Li, L. Occupant behavior effects on energy-saving measures and thermal comfort in severe cold areas. *Energy Sustain. Dev.* **2023**, *73*, 1–12. [[CrossRef](#)]
4. Munckton, B.; Rajagopalan, P. Interaction between Thermal Conditions and Ventilation in Kindergartens in Melbourne, Australia. *Sustainability* **2024**, *16*, 1186. [[CrossRef](#)]
5. Borghero, L.; Clèries, E.; Péan, T.; Ortiz, J.; Salom, J. Comparing Cooling Strategies to Assess Thermal Comfort Resilience of Residential Buildings in Barcelona for Present and Future Heatwaves. *Build. Environ.* **2023**, *231*, 110043. [[CrossRef](#)]
6. Prieto, A.; Knaack, U.; Auer, T.; Klein, T. Passive Cooling & Climate Responsive Façade Design: Exploring the Limits of Passive Cooling Strategies to Improve the Performance of Commercial Buildings in Warm Climates. *Energy Build.* **2018**, *175*, 30–47. [[CrossRef](#)]
7. Iskandar, L.; Bay-Sahin, E.; Martinez-Molina, A.; Beeson, S. Evaluation of Passive Cooling Through Natural Ventilation Strategies in Historic Residential Buildings Using CFD Simulations. *Energy Build.* **2024**, *308*, 114005. [[CrossRef](#)]
8. Prieto, A.; Knaack, U.; Klein, T.; Auer, T. 25 Years of Cooling Research in Office Buildings: Review for the Integration of Cooling Strategies into the Building Façade (1990–2014). *Renew. Sustain. Energy Rev.* **2017**, *71*, 89–102. [[CrossRef](#)]
9. Lapisa, R.; Bozonnet, E.; Salagnac, P.; Abadie, M. Optimized Design of Low-Rise Commercial Buildings Under Various Climates—Energy Performance and Passive Cooling Strategies. *Build. Environ.* **2018**, *132*, 83–95. [[CrossRef](#)]
10. Taleb, H. Using Passive Cooling Strategies to Improve Thermal Performance and Reduce Energy Consumption of Residential Buildings in U.A.E. Buildings. *Front. Archit. Res.* **2014**, *3*, 154–165. [[CrossRef](#)]
11. Gilvaei, Z.; Poshtiri, A.; Akbarpoor, A. A Novel Passive System for Providing Natural Ventilation and Passive Cooling: Evaluating Thermal Comfort and Building Energy. *Renew. Energy* **2022**, *198*, 463–483. [[CrossRef](#)]
12. Belmonte, M.; Díaz-López, C.; Gavilanes, J.; Milán, E. Introducing Passive Strategies in the Initial Stage of the Design to Reduce the Energy Demand in Single-Family Dwellings. *Build. Environ.* **2021**, *197*, 107832. [[CrossRef](#)]
13. Hu, M.; Zhang, K.; Nguyen, Q.; Tasdizen, T. The Effects of Passive Design on Indoor Thermal Comfort and Energy Savings for Residential Buildings in Hot Climates: A Systematic Review. *Urban Clim.* **2023**, *49*, 101466. [[CrossRef](#)]
14. Bhamare, D.; Rathod, M.; Banerjee, J. Passive cooling techniques for building and their applicability in different climatic zones—The state of art. *Energy Build.* **2019**, *198*, 467–490. [[CrossRef](#)]
15. Alkaragoly, M.; Maerefat, M.; Targhi, M. A Novel Hybrid Passive Cooling System for Providing Thermal Comfort Conditions and Reducing Energy Consumption in Buildings in Hot Climates. *Renew. Energy* **2024**, *234*, 121209. [[CrossRef](#)]
16. Fanger, P. *Thermal Comfort: Analysis and Applications in Environmental Engineering*; Danish Technical Press: Copenhagen, Denmark, 1970.
17. ANSI/ASHRAE Standard-55; Thermal Environmental Conditions for Human Occupancy. American Society of Heating, Refrigerating and Air-Conditioning Engineers: Atlanta, GA, USA, 2017.

18. ISO 7730:2005; Ergonomics of the Thermal Environment Analytical Determination and Interpretation of Thermal Comfort Using Calculation of the PMV and PPD Indices and Local Thermal Comfort Criteria. ISO: Geneva, Switzerland, 2005.
19. Shao, T. Indoor Environment Intelligent Control System of Green Building Based on PMV Index. *Adv. Civ. Eng.* **2021**, *2021*, 6619401. [[CrossRef](#)]
20. Khechiba, A.; Djaghroui, D.; Benabbas, M.; Leccese, F.; Rocca, M.; Salvadori, G. Balancing Thermal Comfort and Energy Consumption in Residential Buildings of Desert Areas: Impact of Passive Strategies. *Sustainability* **2023**, *15*, 8383. [[CrossRef](#)]
21. Laouadi, A. A New General Formulation for the PMV Thermal Comfort Index. *Buildings* **2022**, *12*, 1572. [[CrossRef](#)]
22. Faraji, A.; Rashidi, M.; Rezaei, F.; Rahnamayiezekavat, P. A Meta-Synthesis Review of Occupant Comfort Assessment in Buildings (2002–2022). *Sustainability* **2023**, *15*, 4303. [[CrossRef](#)]
23. Omidvar, A.; Kim, J. Modification of Sweat Evaporative Heat Loss in The PMV/PPD Model to Improve Thermal Comfort Prediction in Warm Climates. *Build. Environ.* **2020**, *176*, 106868. [[CrossRef](#)]
24. Doherty, T.; Arens, E. Evaluation of the Physiological Bases of Thermal Comfort Models. *ASHRAE Trans.* **1988**, *94*, 1371–1385.
25. Kähkönen, E. Draught, Radiant Temperature Asymmetry and Air Temperature—A Comparison Between Measured and Estimated Thermal Parameters. *Indoor Air* **1991**, *1*, 439–447. [[CrossRef](#)]
26. Parsons, K. The Effects of Gender, Acclimation State, the Opportunity to Adjust Clothing and Physical Disability on Requirements for Thermal Comfort. *Energy Build.* **2002**, *34*, 593–599. [[CrossRef](#)]
27. Fanger, P.; Toftum, J. Extension of the PMV Model to Non-Air-Conditioned Buildings in Warm Climates. *Energy Build.* **2002**, *34*, 533–536. [[CrossRef](#)]
28. Alfano, F.; Ianniello, E.; Palella, B. PMV–PPD and Acceptability in Naturally Ventilated Schools. *Build. Environ.* **2013**, *67*, 129–137. [[CrossRef](#)]
29. Kim, J.; de Dear, R. Thermal Comfort Expectations and Adaptive Behavioural Characteristics of Primary and Secondary School Students. *Build. Environ.* **2018**, *127*, 13–22. [[CrossRef](#)]
30. Zang, X.; Liu, K.; Qian, Y.; Qu, G.; Yuan, Y.; Ren, L.; Liu, G. The Influence of Different Functional Areas on Customers’ Thermal Comfort—A Field Study in Shopping Complexes of North China. *Energy Built Environ.* **2023**, *4*, 297–307. [[CrossRef](#)]
31. Du, C.; Li, B.; Cheng, Y.; Li, C.; Liu, H.; Yao, R. Influence of Human Thermal Adaptation and Its Development on Human Thermal Responses to Warm Environments. *Build. Environ.* **2018**, *139*, 134–145. [[CrossRef](#)]
32. Yao, R.; Li, B.; Liu, J. A Theoretical Adaptive Model of Thermal Comfort–Adaptive Predicted Mean Vote (aPMV). *Build. Environ.* **2009**, *44*, 2089–2096. [[CrossRef](#)]
33. Zhang, S.; Cheng, Y.; Fang, Z.; Lin, Z. Improved Algorithm for Adaptive Coefficient of Adaptive Predicted Mean Vote (aPMV). *Build. Environ.* **2019**, *163*, 106318. [[CrossRef](#)]
34. Carlucci, S.; Bai, L.; de Dear, R.; Yang, L. Review of Adaptive Thermal Comfort Models in Built Environmental Regulatory Documents. *Build. Environ.* **2018**, *137*, 73–89. [[CrossRef](#)]
35. ANSI/ASHRAE Standard 62-1; Ventilation for Acceptable Indoor Air Quality. American Society of Heating, Refrigerating and Air-Conditioning Engineers: Atlanta, GA, USA, 2022.
36. Miao, S.; Gangolells, M.; Tejedor, B. Data-driven Model for Predicting Indoor Air Quality and Thermal Comfort Levels in Naturally Ventilated Educational Buildings Using Easily Accessible Data for Schools. *J. Build. Eng.* **2023**, *80*, 108001. [[CrossRef](#)]
37. Miao, S.; Gangolells, M.; Tejedor, B. A Comprehensive Assessment of Indoor Air Quality and Thermal Comfort in Educational Buildings in the Mediterranean Climate. *Indoor Air* **2023**, *2023*, 6649829. [[CrossRef](#)]
38. Makaveckas, T.; Bliūdžius, R.; Alavočienė, S.; Paukštys, V.; Brazionienė, I. Investigation of Microclimate Parameter Assurance in Schools with Natural Ventilation Systems. *Buildings* **2023**, *13*, 1807. [[CrossRef](#)]
39. Tran, M.T.; Wei, W.; Dasonville, C.; Martinsons, C.; Ducruet, P.; Mandin, C.; Héquet, V.; Wargocki, P. Review of Parameters Measured to Characterize Classrooms’ Indoor Environmental Quality. *Buildings* **2023**, *13*, 433. [[CrossRef](#)]
40. Voss, K.; Voß, T.; Kaliga, M. Indoor Climate Monitoring in Office Buildings—Comparative Analysis of Two Office Buildings without Air Conditioning. *Energies* **2023**, *16*, 6790. [[CrossRef](#)]
41. Tam, C.; Zhao, Y.; Liao, Z.; Zhao, L. Mitigation Strategies for Overheating and High Carbon Dioxide Concentration within Institutional Buildings: A Case Study in Toronto, Canada. *Buildings* **2020**, *10*, 124. [[CrossRef](#)]
42. Hattori, S.; Iwamatsu, T.; Miura, T.; Tsutsumi, F.; Tanaka, N. Investigation of Indoor Air Quality in Residential Buildings by Measuring CO₂ Concentration and a Questionnaire Survey. *Sensors* **2022**, *22*, 7331. [[CrossRef](#)]
43. Zhang, J.; Chan, C.; Kwok, H.; Cheng, J. Multi-indicator Adaptive HVAC Control System for Low-Energy Indoor Air Quality Management of Heritage Building Preservation. *Build. Environ.* **2023**, *246*, 110910. [[CrossRef](#)]
44. Kumar, K.; Saboor, S.; Kumar, V.; Kim, K.; Babu, A. Experimental and Theoretical Studies of Various Solar Control Window Glasses for The Reduction of Cooling and Heating Loads in Buildings Across Different Climatic Regions. *Energy Build.* **2018**, *173*, 326–336. [[CrossRef](#)]
45. Kalmár, F.; Kalmár, T. Thermal Comfort Aspects of Solar Gains during the Heating Season. *Energies* **2020**, *13*, 1702. [[CrossRef](#)]
46. Koç, S.; Kalfa, S. The Effects of Shading Devices on Office Building Energy Performance in Mediterranean Climate Regions. *J. Build. Eng.* **2021**, *44*, 102653. [[CrossRef](#)]
47. Mohammed, A.; Tariq, M.A.U.R.; Ng, A.W.M.; Zaheer, Z.; Sadeq, S.; Mohammed, M.; Mehdizadeh-Rad, H. Reducing the Cooling Loads of Buildings Using Shading Devices: A Case Study in Darwin. *Sustainability* **2022**, *14*, 3775. [[CrossRef](#)]

48. Qin, S.; Liu, Y.; Yu, G.; Li, R. Assessing the Potential of Integrated Shading Devices to Mitigate Overheating Risk in University Buildings in Severe Cold Regions of China: A Case Study in Harbin. *Energies* **2023**, *16*, 6259. [[CrossRef](#)]
49. Hernández, F.; López, J.; Suárez, J.; Muriano, M.; Rueda, S. Effects of Louvers Shading Devices on Visual Comfort and Energy Demand of an Office Building. A Case of Study. *Energy Procedia* **2017**, *140*, 2017–2216. [[CrossRef](#)]
50. Pérez-Carramiñana, C.; González-Avilés, Á.B.; Castilla, N.; Galiano-Garrigós, A. Influence of Sun Shading Devices on Energy Efficiency, Thermal Comfort and Lighting Comfort in a Warm Semi-Arid Dry Mediterranean Climate. *Buildings* **2024**, *14*, 556. [[CrossRef](#)]
51. Lizana, J.; Chacartegui, R.; Barrios-Padura, A.; Ortiz, C. Advanced Low-Carbon Energy Measures Based on Thermal Energy Storage in Buildings: A Review. *Renew. Sustain. Energy Rev.* **2018**, *82*, 3705–3749. [[CrossRef](#)]
52. Layeni, A.; Waheed, M.; Adewumi, B.; Bolaji, B.; Nwaokocha, C.; Giwa, S. Computational Modelling and Simulation of the Feasibility of a Novel Dual Purpose Solar Chimney for Power Generation and Passive Ventilation in Buildings. *Sci. Afr.* **2020**, *8*, e00298. [[CrossRef](#)]
53. Moghaddam, H.; Tkachenko, S.; Yeoh, G.; Timchenko, V. A Newly Designed BIPV System with Enhanced Passive Cooling and Ventilation. *Build. Simul.* **2023**, *16*, 2093–2107. [[CrossRef](#)]
54. Fawwaz Alrebei, O.; Obeidat, L.M.; Ma'bdeh, S.N.; Kaouri, K.; Al-Radaideh, T.; Amhamed, A.I. Window-Windcatcher for Enhanced Thermal Comfort, Natural Ventilation and Reduced COVID-19 Transmission. *Buildings* **2022**, *12*, 791. [[CrossRef](#)]
55. Heidari, S.; Poshtiri, A.; Gilvaei, Z. Enhancing Thermal Comfort and Natural Ventilation in Residential Buildings: A Design and Assessment of an Integrated System with Horizontal Windcatcher and Evaporative Cooling Channels. *Energy* **2024**, *289*, 130040. [[CrossRef](#)]
56. Maask, V.; Rosin, A.; Korôtko, T.; Thalfeldt, M.; Syri, S.; Ahmadiyahangar, R. Aggregation Ready Flexibility Management Methods for Mechanical Ventilation Systems in Buildings. *Energy Build.* **2023**, *296*, 113369. [[CrossRef](#)]
57. Hou, F.; Ma, J.; Kwok, H.; Cheng, J. Prediction and Optimization of Thermal Comfort, IAQ and Energy Consumption of Typical Air-Conditioned Rooms Based On a Hybrid Prediction Model. *Build. Environ.* **2022**, *225*, 109576. [[CrossRef](#)]
58. Conceição, E.; Lúcio, M. Numerical Simulation of Passive and Active Solar Strategies in Buildings with Complex Topology. *Build. Simul.* **2010**, *3*, 245–261. [[CrossRef](#)]
59. Conceição, E.; Gomes, J.; Awbi, H. Influence of the Airflow in a Solar Passive Building on the Indoor Air Quality and Thermal Comfort Levels. *Atmosphere* **2019**, *10*, 766. [[CrossRef](#)]
60. Conceição, M.I.; Conceição, E.; Lúcio, M.; Gomes, J.; Awbi, H. Application of Semi-Circular Double-Skin Facades in Auditoriums in Winter Conditions. *Inventions* **2023**, *8*, 60. [[CrossRef](#)]
61. Aish, R.; Vuren, J.; Walmsley, M. Integrated CAD Development for Building Services Engineering. *Comput. Aided Des.* **1985**, *17*, 179–190. [[CrossRef](#)]
62. Jablonska, J.; Czajka, R. CAD Tools and Computing in Architectural and Urban Acoustics. *Buildings* **2021**, *11*, 235. [[CrossRef](#)]
63. Conceição, E.; Lúcio, M. Numerical Simulation of the Application of Solar Radiant Systems, Internal Airflow and Occupants' Presence in the Improvement of Comfort in Winter Conditions. *Buildings* **2016**, *6*, 38. [[CrossRef](#)]
64. Conceição, E.; Gomes, J.; Lúcio, M.M.; Conceição, M.I.; Awbi, H. Comparative Study of a Clean Technology Based on DSF Use in Occupied Buildings for Improving Comfort in Winter. *Clean Technol.* **2021**, *3*, 311–334. [[CrossRef](#)]
65. Cheng, Y.; Lin, Z.; Fong, A. Effects of Temperature and Supply Airflow Rate on Thermal Comfort in a Stratum-Ventilated Room. *Build. Environ.* **2015**, *92*, 269–277. [[CrossRef](#)]
66. Persily, A. Field measurement of ventilation rates. *Indoor Air* **2016**, *26*, 97–111. [[CrossRef](#)] [[PubMed](#)]
67. Mancini, F.; Nardecchia, F.; Groppi, D.; Ruperto, F.; Romeo, C. Indoor Environmental Quality Analysis for Optimizing Energy Consumptions Varying Air Ventilation Rates. *Sustainability* **2020**, *12*, 482. [[CrossRef](#)]
68. RECS. Regulamento de Desempenho Energético dos Edifícios de Comércio e Serviços (RECS)—Requisitos de Ventilação e Qualidade do Ar Interior—Portaria no 353-A/2013 de 4 de Dezembro. Diário República, 2013; 1ª série 245. 6644-(2)–6644-(9). Available online: <https://diariodarepublica.pt/dr/detalhe/portaria/353-a-2013-331868> (accessed on 12 September 2024). (In Portuguese)
69. Conceição, E.; Silva, A.; Lúcio, M. Numerical Study of Thermal Response of School Buildings in Winter Conditions. In Proceedings of the 9th Conference on Air Distribution in Rooms (Roomvent 2004), Coimbra, Portugal, 5–8 September 2004.
70. Conceição, E.; Lúcio, M. Numerical Study of Thermal Response of School Buildings in Summer Conditions. In Proceedings of the 8th International Conference and Exhibition on Healthy Buildings (HB 2006), Lisbon, Portugal, 4–8 June 2006.
71. Alfano, F.; Pepe, D.; Ricio, G.; Vio, M.; Palella, B. On the effects of the mean radiant temperature evaluation in the assessment of thermal comfort by dynamic energy simulation tools. *Build. Environ.* **2023**, *236*, 110254. [[CrossRef](#)]
72. Lee, D.; Jo, J. Measuring and implementing mean radiant temperature in buildings: Technical review. *Renew. Sustain. Energy Rev.* **2025**, *207*, 114908. [[CrossRef](#)]
73. Mayrhofer, L.; Müller, A.; Bügelmayer-Blaschek, M.; Malla, A.; Kranzl, L. Modelling the Effect of passive Cooling Measures on Future Energy Needs for The Austrian Building Stock. *Energy Build.* **2023**, *296*, 113333. [[CrossRef](#)]
74. Fortin, R.; Mandal, J.; Raman, A.; Craig, S. Passive Radiative Cooling to Sub-Ambient Temperatures Inside Naturally Ventilated Buildings. *Cell Rep. Phys. Sci.* **2023**, *4*, 101570. [[CrossRef](#)]

-
75. Chen, J.; Lu, L.; Gong, Q. Techno-economic and Environmental Evaluation on Radiative Sky Cooling-Based Novel Passive Envelope Strategies to Achieve Building Sustainability and Carbon Neutrality. *Appl. Energy* **2023**, *349*, 121679. [[CrossRef](#)]
 76. Palma, R.; Medina, D.; Delgado, C.; Ramos, J.; Montero-Gutiérrez, P.; Domínguez, S. Enhancing the Building Resilience in a Changing Climate Through a Passive Cooling Roof: A Case Study in Camas (Seville, Spain). *Energy Build.* **2024**, *321*, 114680. [[CrossRef](#)]

Disclaimer/Publisher's Note: The statements, opinions and data contained in all publications are solely those of the individual author(s) and contributor(s) and not of MDPI and/or the editor(s). MDPI and/or the editor(s) disclaim responsibility for any injury to people or property resulting from any ideas, methods, instructions or products referred to in the content.